Distribution Agreement

In presenting this thesis as a partial fulfillment of the requirements for a degree from Emory University, I hereby grant to Emory University and its agents the non-exclusive license to archive, make accessible, and display my thesis in whole or in part in all forms of media, now or hereafter now, including display on the World Wide Web. I understand that I may select some access restrictions as part of the online submission of this thesis. I retain all ownership rights to the copyright of the thesis. I also retain the right to use in future works (such as articles or books) all or part of this thesis.

Nabiha Saklayen April 17, 2012

Confinement of Colloidal Suspensions in Cylindrical Geometries and the Decoupling of Rotational and Translational Diffusion in a 2D Granular Experiment

by

Nabiha Saklayen

Dr. Eric Weeks
Adviser

Department of Physics

Dr. Eric Weeks

Adviser

Dr. Connie Roth

Committee Member

Dr. Leah Roesch

Committee Member

2012

Confinement of Colloidal Suspensions in Cylindrical Geometries and the Decoupling of Rotational and Translational Diffusion in a 2D Granular Experiment

By

Nabiha Saklayen

Dr. Eric Weeks

Adviser

An abstract of
a thesis submitted to the Faculty of Emory College of Arts and Sciences
of Emory University in partial fulfillment
of the requirements of the degree of
Bachelor of Sciences with Honors

Department of Physics

2012

Abstract

Confinement of Colloidal Suspensions in Cylindrical Geometries and the Decoupling of Rotational and Translational Diffusion in a 2D Granular Experiment

By Nabiha Saklayen

We study binary colloidal suspensions confined within a glass microcapillary to model the glass transition in confined cylindrical geometries. We use high speed three-dimensional confocal microscopy to observe particle dynamics. The use of a slightly tapered microcapillary enables us to probe a range of local volumes for a single colloidal sample. We observe that confinement of the sample slows down particles. In addition, the particles form layers against the capillary walls; these layers also influence particle mobility. We split the mobility into three components and see that all components slow down close to the boundary. As the microcapillary is made smaller, all three components of mobility start to show large fluctuations due to the closely packed layers that form in tight spaces. We found that when the volume fraction is increased, the “bulk” mobility of the system decreases.

We also experimentally study the rotation and diffusion of granular clusters in a 2D binary granular system. Our apparatus vibrates a 2D system of densely packed granular bidisperse disks (to avoid crystallization) containing a trackable 3-particle cluster. We use this system to mimic hard-sphere fluids and the clusters probe the system's local translational and rotational dynamics. As the area fraction of the bidisperse disks is increased, diffusion within the sample becomes slower, and above a critical area fraction, the sample behaves as a granular glass. We analyze the rotational and translational motions of the clusters to determine whether they decouple with changing area fraction of the system. As we approach the glass transition, we observe a decoupling between the two motions.

Confinement of Colloidal Suspensions in Cylindrical Geometries and the Decoupling of Rotational and Translational Diffusion in a 2D Granular Experiment

By

Nabiha Saklayen

Dr. Eric Weeks

Adviser

A thesis submitted to the Faculty of Emory College of Arts and Sciences
of Emory University in partial fulfillment
of the requirements of the degree of
Bachelor of Sciences with Honors

Department of Physics

2012

Acknowledgements

Thank you to Eric Weeks for being the most incredible mentor any student could dream of and believing in me every step of the way.

Thank you to my wonderful parents for always whole-heartedly supporting my physics aspirations.

Thank you to Gary Hunter for teaching me everything I know about research, its successes and failures.

Thank you to Leah Roesch and Connie Roth for being on my committee and showing me that women can be amazing scientists too.

Table of Contents

List of Figures

Chapter 1

Introduction

1.1 Jamming and the Glass Transition

Our ideas about what it means to be a solid, liquid, or gas are completely challenged when we encounter everyday materials like toothpaste or peanut butter. These substances are a mixture of solids and liquids and we use the phrase "soft materials" to describe them. Soft materials act as solids at a macroscopic level and have random particle arrangements at a microscopic level. So why are we interested in studying these materials? If you look around you at any given moment, you will see that everything from your computer screen to bottom of your shoe is made of some type of glassy material. Glassy materials are abundant in the natural, industrial, and technological worlds, and we still do not understand why these amorphous materials are solid. The field of soft condensed matter tries to gain a better understanding of these systems,

and glass is one such system that we study. Even though itself glass is a widely used material, we still do not have a full understanding of why this solid is amorphous and not crystalline.

There is no doubt that glass, say in the form of window glass, is a solid in terms of its macroscopic properties. However, the minute you zoom in close to see the underlying atomic structure, you will see that the atoms are completely disordered. Glass has an amorphous solid state with randomly packed atoms, and other similar materials include sand, cotton candy and polystyrene, to name a few examples. We think that understanding the mysterious nature of the glass transition is important because something interesting must be happening that allows solid glass to remain amorphous

The phase of the material, whether it is a glass, liquid, or crystal, is dependent on the complex interactions between the particles. We are interested in knowing what causes the different phases to arise. Perhaps the key to understanding these structural properties lies in studying how glassy solids are formed because the formation process will determine many properties of the glass (Debenedetti and Stillinger 2001). The best way to form a glass is to rapidly cool a viscous liquid (supercooling) and override the crystallization phase. We are interested in what exactly happens during the supercooling process that allows glass to remain amorphous in the glassy state.

One popular approach has been to think of the process in terms of "jamming," a term popularized in this field by Liu and Nagel (1998). A jammed system can be compared to say a traffic jam or a clogged pipe, where the particles get more and more tightly packed together and slows down the system. Eventually the particles get stuck and form a solid structure. Jammed materials are amorphous, meaning that they are structurally disordered and possess a yield stress, which is the pressure that the substance can tolerate without deforming (Weeks

2007). It is speculated that there could exist a universal jammed state that explains the behavior of all amorphous materials that we know of, such as foams, glasses, and emulsions.

The glass transition occurs when the temperature of the glass is lowered so that that the material turns from a liquid to a solid while retaining its microscopically disordered structure. Another way to make a sample undergo a glass transition would be to increase pressure on the system. The viscosity of a fluid is a measure of a fluid's resistance to flow, which is low for hot liquid glass as it flows very easily. When the liquid is cooled towards the glass transition, a change in temperature of just a few tens of degrees causes a remarkably dramatic rise in its viscosity by 10 or more orders of magnitude (Weeks 2007). Eventually the viscosity becomes so large that the molecular motion comes to a complete halt and the glassy state becomes "jammed."

This thesis looks to specifically explore our understanding of the glass transition in two different ways, and I use two different hard-sphere models to study the glass transition. One is a colloidal suspension and the other is a granular two-dimensional disk system. Hard-sphere models help us increase our understanding of liquids. A hard-sphere model can be defined as a collection of perfect spheres that interact with zero potential unless they overlap, in which case the potential becomes infinitely large. The key point is that the particles cannot overlap under any circumstances and their behavior is similar to that of a collection of hard marbles. Particles in colloidal suspensions and granular systems act just like hard spheres, which makes them desirable model systems to study the glass transition in more depth.

1.2 Confinement of Colloids

The first experiment uses colloids to study the glass transition. Colloids have evolved to become a very popular model system to study the glass transition, and they can be used in a variety of

different ways to probe glassy systems. They are a simple yet effective model system because the particles are large enough to be imaged using microscopy techniques, yet small enough to perform random Brownian motion. The biggest advantage is that particle behavior can be investigated in great detail using advanced microscopy techniques, such as the 3D confocal microscopy technique that I use in this thesis. The particle size allows us to track the particles easily due to their significantly lower mobility than an atom or a molecule. Instead of changing the temperature or pressure to achieve the glass transition in a colloid, we change the volume fraction for the same effect. The volume fraction is a measure of how densely the particles are packed together, and is calculated by dividing the total volume of particles by the total volume of the system. The only thing that needs to be changed to alter the system's glassiness is the number of particles in the system, in other words the volume fraction, which is done fairly easily by centrifugation. We centrifuge our samples to sediment the particles and then remove or add solvent to change the total volume fraction of the sample.

Even though we have an increased understanding of how different factors contribute to the glass transition, we still unfortunately do not have a complete understanding of this phenomenon. The glass transition becomes even more interesting when materials are restricted to uncomfortably small spaces. When glassy materials are confined in small spaces, they begin to exhibit properties different from their bulk properties. Glassy materials have been confined in nanopores and ultrathin polymer films (Alcoutlabi and McKenna 2005; Kim *et al.* 2008) and these various experiments have seen contrasting results, namely, both increased and decreased amounts of glassiness. The disparities in experimental results make clear that the glass transition is heavily dependent on the specific experimental details used at that instant. This realization has inspired soft condensed matter physicists to devise new experiments that expand our understanding of confined glassy materials in new and exciting directions.

The confinement effect on glass transition can be studied in different materials and systems, and I study the colloidal glass transition in confinement in this thesis. Colloidal suspensions are our model of choice and we confine them in restricted spaces of different geometries. Colloids have been previously confined in one dimension between parallel plates (Nugent *et al.* 2007) to give interesting results. Colloidal suspensions of constant density were confined between plates of varying width, and the particles were seen to slow down as they were confined to narrower channels. These experiments have also suggested that the boundary conditions, which would be the walls of the parallel plates in this case, play an important role in triggering the glass transition (Edmond *et al.* 2010). These results show that colloidal particles exhibit different properties depending on the amount of space they have and the nature of the nearest boundaries. There seem to be several aspects of the story that we do not understand, and we want to increase our understanding of the confinement effect by confining samples inside spaces of different geometries.

In the first part of this thesis, I study colloidal suspensions confined within cylinders, and this experiment models a two-dimensional confinement effect that has not been studied previously. The goal for this experiment is to add another dimension to the one-dimensional confinement effect studied previously (Nugent *et al.* 2007), and study how that influences particle mobility in the system.

1.3 Decoupling of Rotational and Translational Diffusion

The second part of the thesis studies another aspect of the glass transition by using a different, and much larger, model system. When you consider a molecule or particle diffusing through space, you see that the particle is translating through space (moving from one point to another) and also rotating around its center. Since these two motions are happening at the same time

and due to the same physical parameters, it is natural to expect that they would be similar for the same particle. However, it turns out that this is not universally true for all systems, and glassy materials are an exception to the rule.

When molecules are energized at high temperatures, their rotational and translational diffusion coefficients are inversely proportional to the viscosity η of the material. If the two components of diffusion are coupled, they rotate and translate at the same rate. It turns out that when you cool a glassy material to approach T_g, the glass transition temperature, these supercooled liquids show a decoupling of the translational and rotational diffusion (Debenedetti and Stillinger, 2001; Cicerone and Ediger 1996). This means that the rotation slows down more than the translation or, in other words, the particles translate more per individual rotation. The decoupling is perhaps attributed to spatially heterogeneous dynamics in the system, which means that different parts of the sample, even though they are relatively close by, are translating at different rates (Ediger 2000).

The following relationship is important motivation for the experiment:

$$\frac{D_T}{D_R} = constant. \qquad (1.1)$$

In equation (1.1), D_T is the measure of translational motion a particle is undergoing, which simply measures how much the particle is moving around on average. D_R is a measure of how much the particle is spinning around its central axis. For a Newtonian fluid, such as water, D_T/D_R changes in a simple manner when either temperature T or viscosity η are changed. Interestingly enough, the ratio in Eqn. 1.1 always turns out to be a constant value for any given shape being studied in a fluid. For example, for a dramatic drop in viscosity, both types of mobility in the form of D_T and D_R will increase in a similar fashion.

Even though this equation holds true for many fluids, supercooled fluids close to the glass transition do not have a constant D_T/D_R value. Even though both translation and rotation are a result of similar physical parameters, they respond very differently when approaching the glass transition. This discrepancy suggests that we cannot think of supercooled liquids as simple Newtonian fluids, and that perhaps supercooled particles or molecules have intrinsically different diffusion traits. Most previous studies on this topic have found that molecules tend to translate faster than they rotate on approaching the glass transition (Chang *et al.* 1994; Debenedetti and Stillinger 2001) even though some have seen the opposite effect (Holz et al. 1996).

The second part of the thesis studies this behavior in a new hard sphere model system. I built a granular shaker experiment to see how small three-disk clusters (disks~0.5cm in diameter) translate and rotate through a sea of particles at different area fractions (densities) of particles. The rotation of the trimer slows down more than the translation. This is described as a decoupling of the rotational and translational diffusions in this system, which is similar to what has been seen in previous studies (Chang *et al.* 1994; Debenedetti and Stillinger 2001).

1.4 Particle Tracking

Image analysis is a useful tool that allows us to study the underlying dynamics of the system by tracking the motion of individual particles in a colloid (Habdas and Weeks 2002) or a granular system of particles. I used IDL (interactive data language) to analyze the raw data for both of my experiments. The beauty of IDL particle tracking is that it allows us to track the motion of hundreds of particles at the same time (Crocker and Grier 1996). The particle centers are found by computing the brightness-weighted centroid of individual particles and their position can then be determined quite accurately. There are limitations of this technique, such as noise in

the original data or the number of pixels of particles, but the optical resolution of the microscopes are impressive, at about 200 nm for a 100x objective that we would use to study colloids (Habdas and Weeks 2002).

Particle tracking allows us to extract useful information and find patterns in the mobility of particles in the system. We calculate the mean square displacement (MSD) of the particles to obtain an average mobility of the particle over some elapsed time.

$$< \Delta r^2 > = < [r(t + \Delta t) - r(t)]^2 > \qquad (1.2)$$

Equation 1.2 shows the definition for the MSD, which we then plot on a log-log plot and vs. lag time. The slope of a log-log plot should be 1 for diffusive behavior. We can then extract the diffusion coefficient for a sample from the slope of a lin-lin plot (linear axes). This slope on a lin-lin plot is equal to *2nD*, where *n* is the number of dimensions (2 or 3) of the data.

Since we had a binary mixture of particles in our colloids, tracking the smaller 1μm particles accurately for our data analysis was diffcult because they were diffusing really fast. However, the data we obtained by tracking the large particles provides us with interesting confinement results.

Chapter 2

Confinement of Colloidal Suspensions in Cylindrical Geometries

2.1 Experimental Details

Colloids have proven to be effective models that mimic real hard-sphere systems, such as the packing of atoms. A hard-sphere system means that the particles in colloids do not interact with one another beyond their radius and are infinitely repulsive at contact [Alder *et al.* 1970; Woodcock 1981; Speedy 1998]. Colloidal particles can arrange themselves in different ways to form liquids, glasses and crystals, which make them an ideal system to study phase transitions (Habdas and Weeks 2002). These particles are designed to be small enough to still undergo random Brownian motion and exhibit diffusive behavior like atoms and molecules. However,

they are still large enough to be imaged using video microscopy, which allows us to extract valuable information about the particle dynamics underlying the system (Prasad *et al.* 2007).

The single parameter that affects phase behavior in colloids is the volume fraction φ, as shown in Eq. 2.1, which is a non-dimensional number related to the number density n ($n=N/V$ with N as the number of particles and V as the total volume). When φ is close to zero, the dilute system will behave like a gas and as you increase φ, the system begins to behave like a liquid and/or glass.

$$\varphi = \frac{4}{3}\pi a^3 \frac{N}{V} \qquad (2.1)$$

The colloids used in this experiment consisted of poly(methyl methacrylate) (PMMA) spheres coated with a polymer brush layer that sterically stabilizes the particles, preventing them from aggregating (Antl *et al.* 1986). We use a binary colloidal suspension with particles of two different radii, 1.08 μm and 0.532 μm, to avoid crystallization in the sample, as that would hinder the random Brownian motion we are interested in studying. The particles are usually made of long polymer chains that form tight coils in an immiscible liquid and are fluorescently dyed during or after synthesis using rhodamine, which emits light of a different wavelength after absorbing light of a particular wavelength.

It is important to remove the effects of gravity in a colloidal suspension by density matching the colloid with the surrounding fluid. The particles float in a 15% cyclohexyl bromide and 85% decahydronaphthalene (decalin) mixture by percentage weight to achieve the desired density matching. The benefit of this particle solvent mixture is that it allows for density matching, which means that gravity does not affect the mobility of particles. The solvent is also refractive

index matched, which allows us to use light microscopy to observe the particles in motion without distorting the image.

The goal of the experiment was to confine the colloidal suspension inside a cylindrical geometry, as shown in Fig. 2.1(b), and we achieved this by filling the narrowest end of a glass capillary tube as shown in Fig 2.1(a). The capillary tip has slight slope of 1%, and the slight taper does not seem to affect our overall results.

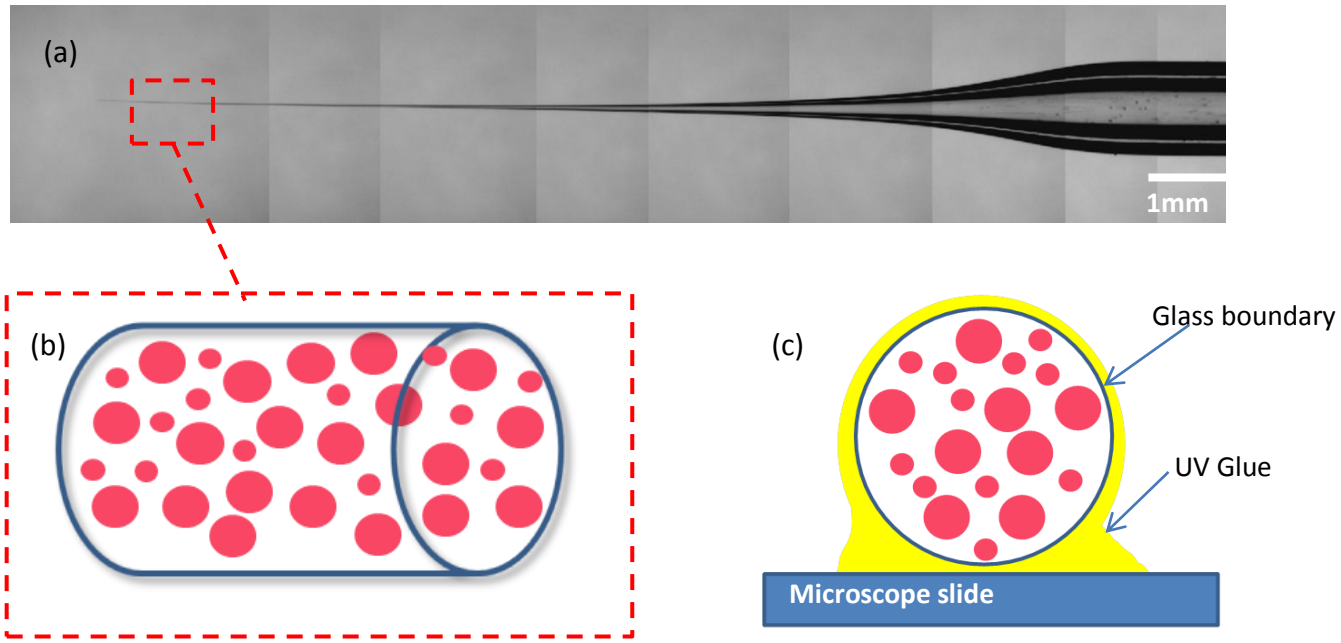

Figure 2.1: Schematic diagram of experimental confinement geometry (a) Image of a narrow capillary glass tip used for the confinement experiment. (b) Colloid confined in a cylindrical geometry. (c) Cross-section of the capillary tip containing colloid.

The capillary tip was made using an automated pipette puller. The end of the capillary tip was cut off by making a slight incision using a scoring tile and then snapping off the large end, while ensuring not to break the thin end of the capillary tube. The shortened capillary tube was then dipped into a vial of binary colloidal suspension for 20 seconds or so, quickly transferred to a microscope slide and glued on by flowing glue over the narrow end of the tube so the open-end tip would be sealed with a thin layer of glue. The colloid travels up the capillary tip due to the

capillary force. We use quick drying UV glue to glue the tip to the slide and a schematic cross-section in Fig. 2.1 (c) shows a thin layer of glue covering the tip all around.

Microscopy is a popular way of imaging colloids because it is easy to use and cost efficient (Prasad *et al.* 2007). We wish to overcome the difficulties posed by multiple scattering or low contrast images from various other forms of microscopy and use laser scanning confocal microscopy (LSCM) to obtain clean data. Confocal microscopy illuminates individual points in the sample and rejects the out of focus light. Laser light hits a fluorescent sample, excites the fluorophores to emit a different color light, passes through a pinhole to remove the out-of-focus light and then is measured by a detector, such as a photomultiplier tube as shown in Fig. 2.2. Individual pixels of data are recorded through the sample and then reconstructed to form 2D slices cutting through the sample. All the 2D slices are merged to form a 3D image of the sample chamber. Being able to create 3D images makes confocal microscopy a powerful tool for studying particle dynamics in the system.

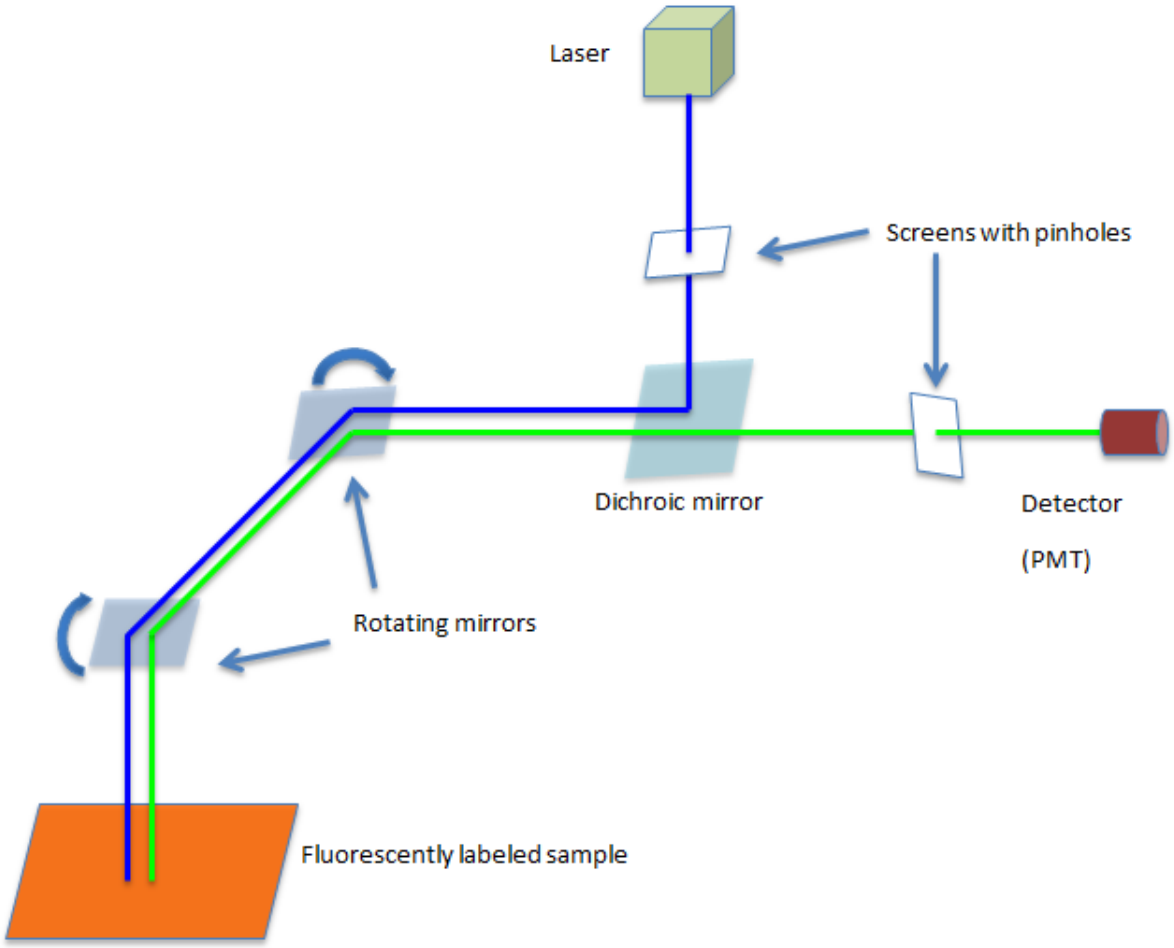

Figure 2.2: Schematic diagram of a conventional confocal microscope.

I imaged different portions of the capillary tube filled with a sample of constant volume fraction φ. I also prepared different tubes with different colloidal suspensions to obtain a range of φ's. The goal was to obtain data from as many samples of different φ's as possible and capture data from a various diameters of the capillary tube for a particular φ.

Confocal microscopy allows us to capture individual images like the one shown in Fig. 2.3 and then render three-dimensional images of the sample. Fig. 2.3 shows an image of a binary mixture with particles of two different diameters confined in a capillary tip, and all the data

analyzed in this thesis looked just like this data shown.

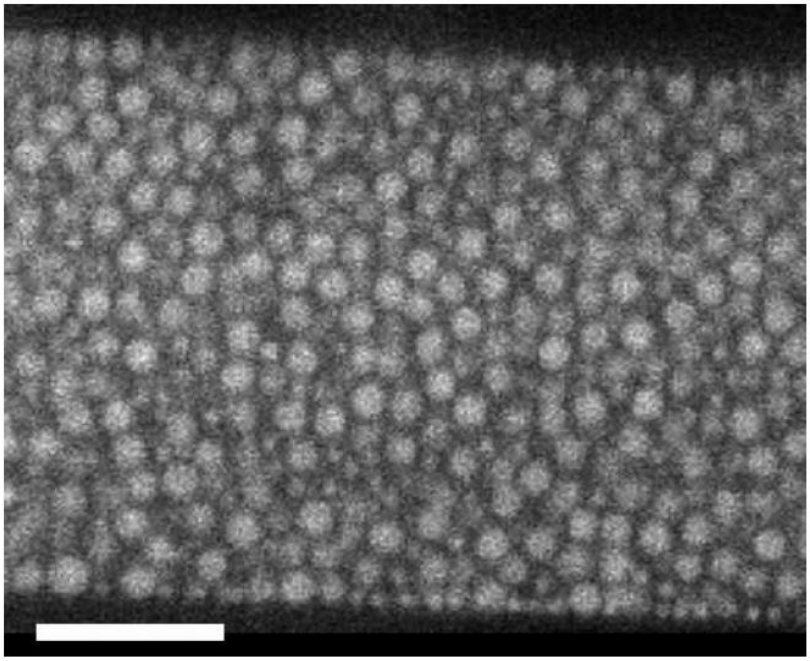

Figure 2.3: Confocal image of a confined binary colloidal suspension inside a capillary tip. The scale bar is 10μm.

As the confocal microscope scans through the sample chamber, it takes snapshots at different heights of the sample, which leads to creation of a 3D image of the entire sample chamber (Prasad *et al.* 2007). In order to illustrate what a 3D image would look like, a 3D rendered image made using Pixar imaging software of the dataset is shown in Fig. 2.4.

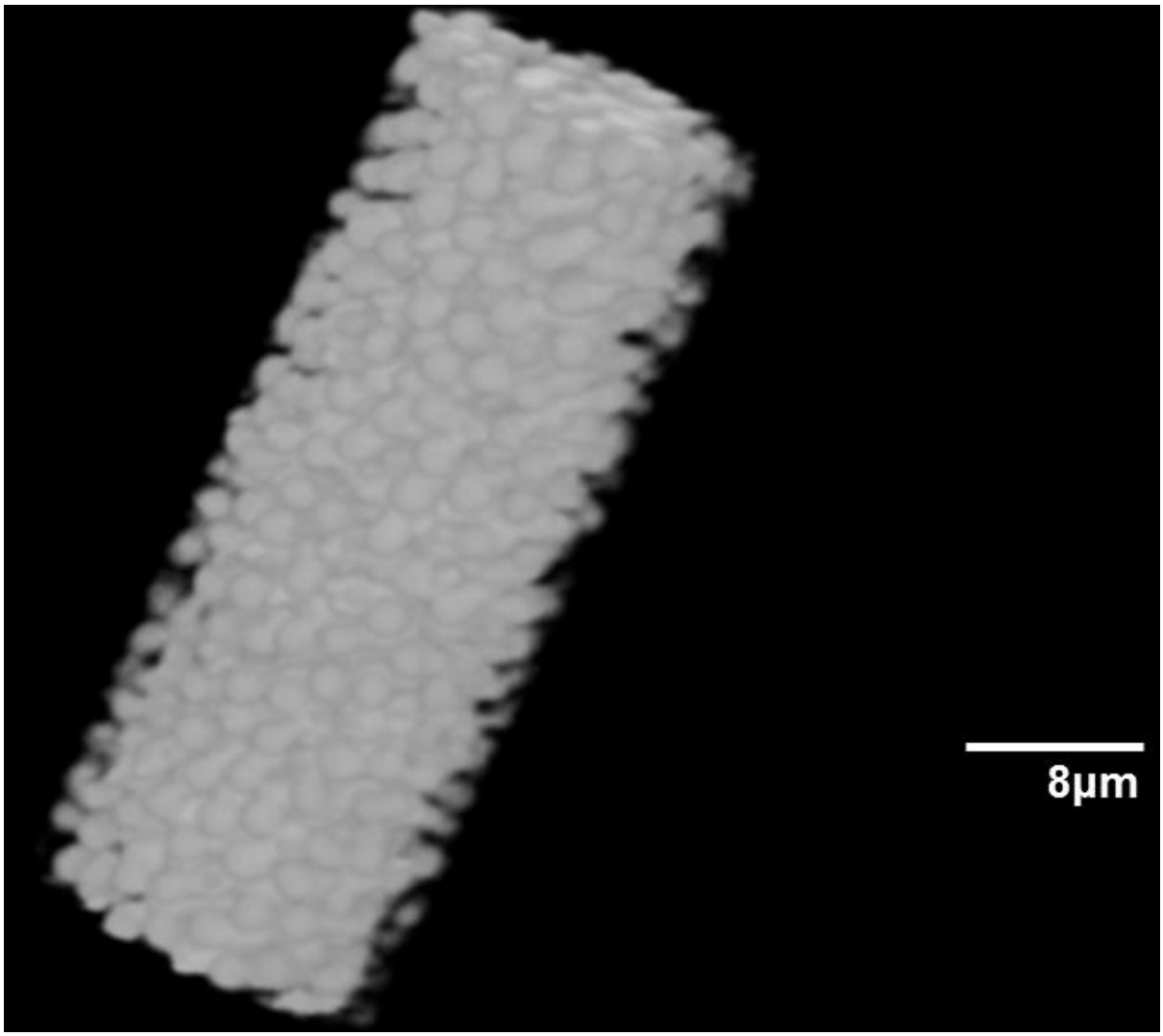

Figure 2.4: 3D rendering of a confocal stack of images shows the cylindrical confinement of the sample.

Each scan takes about 2-3 seconds, and I use the confocal to record 400 of these individual 3D stacks to create essentially a 3D movie of the data for an extended period of time. The advantage of this imaging technique is that each particle can be observed in 3D over short time scales, which allows us to accurately track the location of the particles over time.

2.2 Results

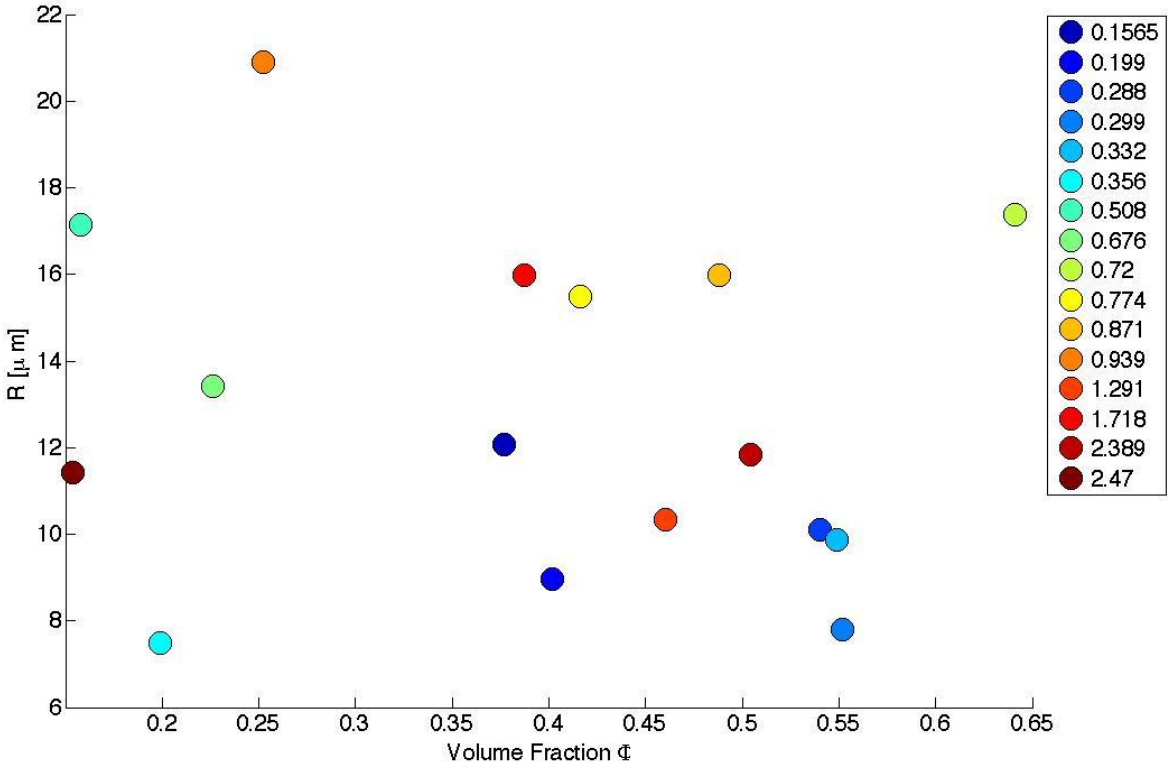

Figure 2.5: Range of datasets used in this thesis with radius of tubes plotted as a function of volume fraction φ, the colors represent the average mean square displacement, which will be discussed later.

Figure 2.5 shows the range of data obtained from this experiment and discussed in this thesis. The y axis plots the radii of the cylinders in μm and the volume fraction φ is plotted along the x axis. The colors on the plots represented average mobility for the particles, which I will describe in more depth shortly. Figure 2.5 simply shows that our data contains a range of volume fractions and radii, and the goal is to find trends in particle behavior is this diverse collection of data. Since the motivation behind the experiment is to observe how particles act in confined places, looking at how far all the particles move over the same timescale becomes important information for us. We know from previous studies that confinement can cause particles to slow

down significantly (Nugent *et al.* 2007), and we want to see if this happens in my 2D confinement system, which is a cylinder in this experiment. All the data analysis is done using IDL software, which is a powerful tool that allows us to analyze the mobility of every single particle in our images.

Since we want to study Brownian motion in mote depth, consider studying a diffusing particle's motion in the x-direction; since the particle has an equal probability of moving to the left or right, the mean displacement of the particle will be zero (Weeks 2010). This will be true for all the particles in the sample, which makes <x>, the mean displacement for all particles, zero as well. However, the mean square displacement (MSD) for the particles will not be zero, and is defined by equation 1.2 in chapter 1. In dilute suspensions, the mean square distance is as follows:

$$\langle \Delta x^2 \rangle = 2D\Delta t \qquad (2.1)$$

In Equation 2.1, D is the diffusion constant, given by the Stokes-Einstein-Sutherland formula for a sphere of radius a:

$$D = \frac{k_B T}{6\pi\eta a} \qquad (2.2)$$

where η is the liquid viscosity (Einstein 1905; Sutherland 1905). When D is larger, the motion of particles is faster. We use MSD curves to analyze particle mobility and they give us valuable insight into what the dynamics are at the molecular scale. Such a MSD plot is shown in Fig. 2.6, where the MSD for three different datasets of similar radii and different ϕ are plotted on the same axes to allow for easier comparison. The green line represents data from least dense cylinder, and the blue and purple lines represent data from denser cylinders. The green line is further up than the others, which means that the MSD plotted on the y-axis is larger for the

green line, and the particles are moving faster in that sample than they are in any other samples. These MSD's are saying that the particles are moving slower as the ϕ increases and the sample becomes denser.

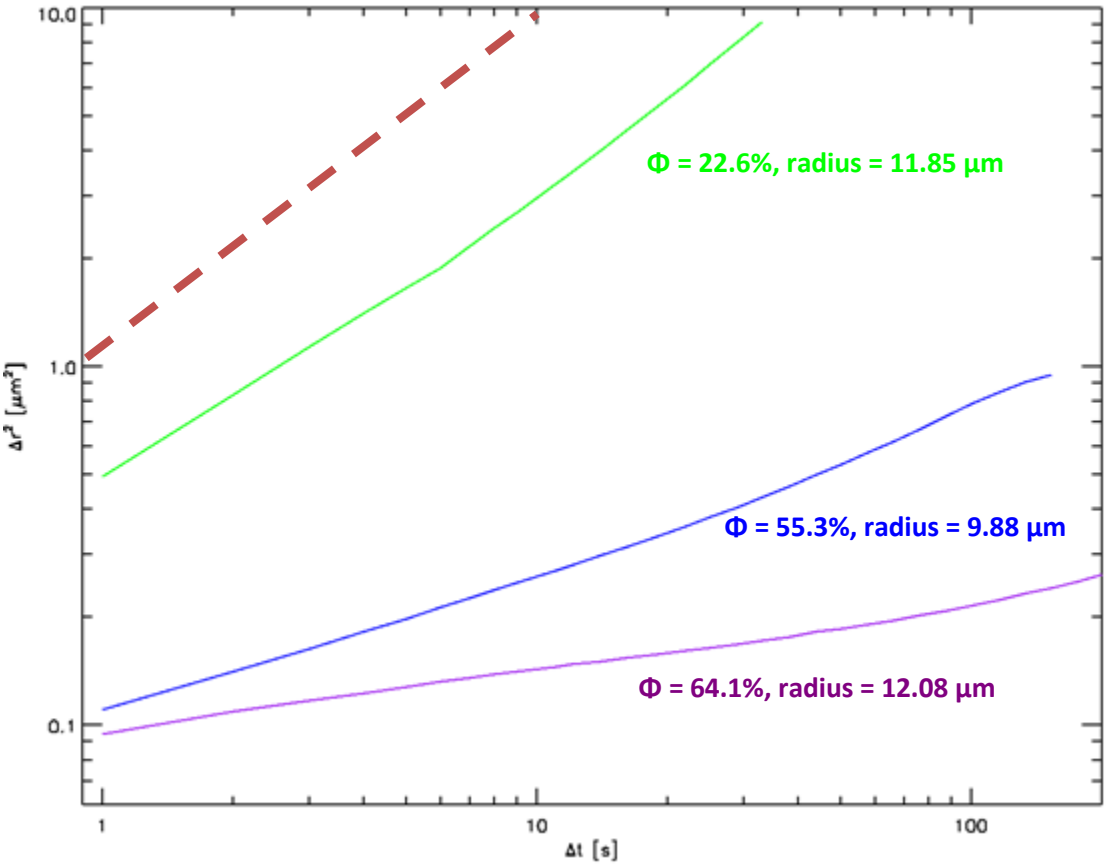

Figure 2.6: Mean square displacement plotted as a function of lag time. The dashed line is there to guide the eye and has a slope of 1, which signifies regular diffusion in a liquid. The ϕ's and radii of the tubes are as follows: green- ϕ =22.6% and radius=11.85μm, blue- ϕ =55.3% and radius=9.88μm, green- ϕ =64.1% and radius=12.08μm.

MSD curves are really useful for data analysis, and we will see more of them throughout the thesis. We can go ahead and extract other useful values from the MSD curves. To get a better sense of what the average mobility is like, we can use IDL to calculate the average mobility of the particles after 30 seconds from an MSD curve (or any amount of time we want) and then plot that against different parameters. Figure 2.7 is plotting the average mobility of particles as a function of volume fraction they are in. The points on the plot show a downward trend

towards the right, suggesting that as the volume fraction is increased, the particles slow down on average. The colors on the plot represent the size of the tube, and the dark blue points represent the smallest tubes. The dark blue points are relatively lower than the other data points, hinting that perhaps the particles are slower in smaller spaces.

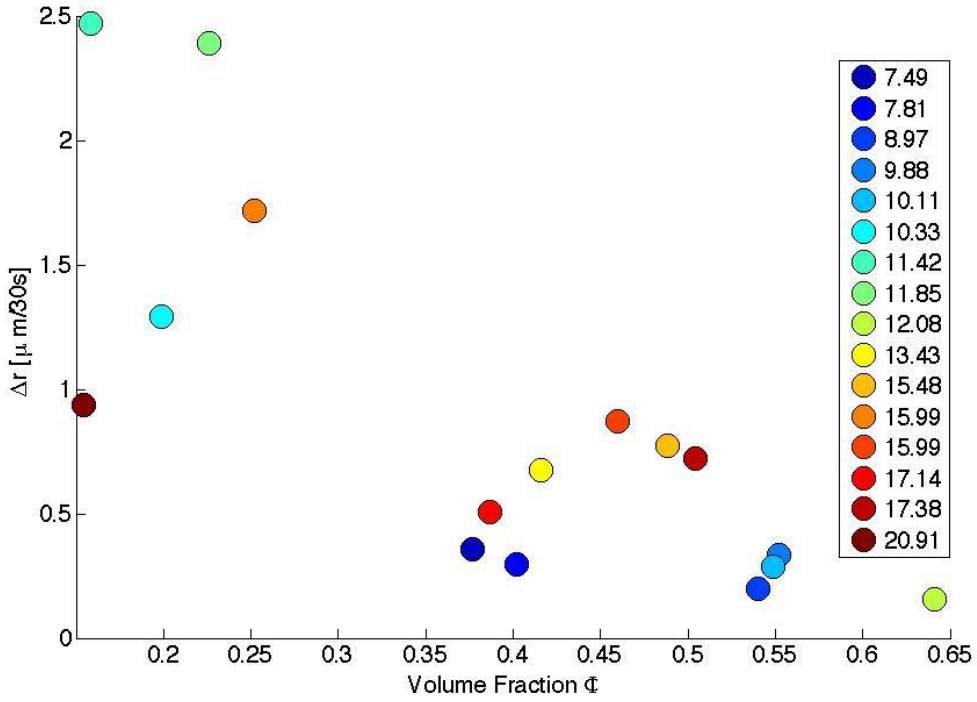

Figure 2.7: Average mobility plotted as a function of volume fraction. The colors represent the tube radius.

We can then go ahead and plot the average mobility as a function of tube size in *μm* as shown in Fig. 2.8, where the colors represent the volume fractions of the samples. There is a downward trend of the data towards the left, suggesting that particles move slower when inside a smaller tube. The blue points are very low volume fractions, and have a much higher overall mobility compared to the other denser samples. The important point to note here is that even though the volume fraction is slightly different for these samples, there is a clear downward trend in the data points.

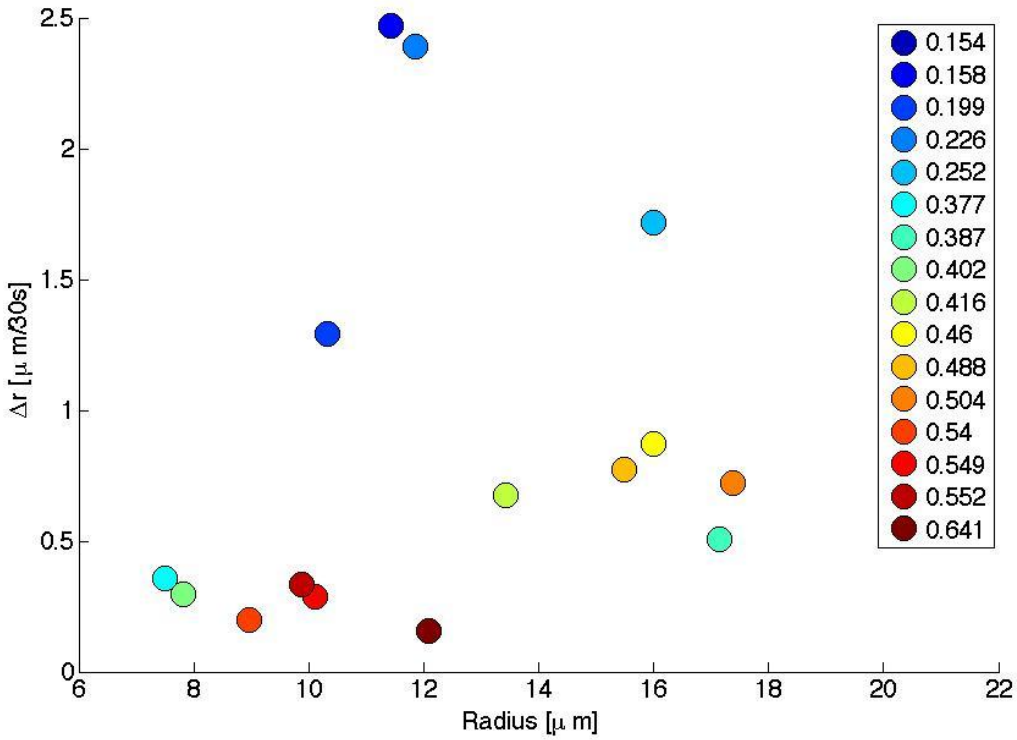

Figure 2.8: Average mobility plotted as a function of tube radius. The colors represent volume fraction.

Even though samples are showing an overall slowing down in mobility, thus reaffirming that approaching the glass transition slows down the average mobility of particles, we want to delve deeper because what we are really interested in is how the dimensions of the system affects mobility. Since we have a cylindrical geometry, we want to see what our specific cylindrical geometry does to mobility. We therefore split up the MSD into three different components, as shown in Fig. 2.9, and we plot these as a function of distance from the boundary of confinement, because we suspect that the components are affected differently based on how far away the particles are from the wall.

The red arrow in Fig. 2.9 shows the axial mobility$<\Delta r_z^2>$ of the particles, which is the mobility up and down the tube. The green line indicates the radial mobility $<\Delta r_S^2>$, which means the particles are moving away from and towards the boundary of confinement. The blue curved

arrow is for angular mobility $<\Delta r_\theta^2>$, which measures how much particles are moving along the curved direction of the cylinder.

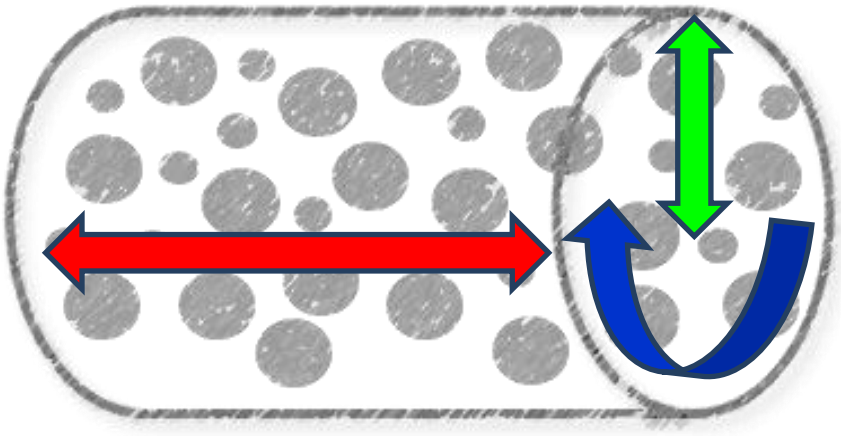

Figure 2.9: Schematic diagram of all the MSD components in a cylindrical geometry. Red is the AXIAL MSD: $<\Delta r_z^2>$, Green is the RADIAL MSD: $<\Delta r_S^2>$, Blue is the ANGULAR MSD: $<\Delta r_\theta^2>$.

Now that we have definitions for three different components of mobility, we can begin to look at those different components. Figure 2.10(b) shows a plot of number density *n(r)* as a function of distance from the confinement boundary for a tube of radius 19.8μm and ϕ=51.4%. Close to the center of the tube, the interior number density is constant at around 0.85μm^{-3}, which is towards the right side on Fig. 2.10(b). When s is about 0.5 μm, there is a small peak in the number density, and moving further away from the wall causes the peaks to get smaller. There are 4 evenly spread out peaks or bumps, suggesting four layers of particles having formed on approaching the boundary. The distance between the local minima of the number density is about 2.3 μm, which suggests that the particles are residing in monolayers, as the larger particles in the binary sample are 2 μm in diameter. The three components of the mean-square displacement of particles for that same tube are plotted in Figure 2.10(a) as a function of distance from the wall of confinement to the center of the tube, and you can see that they all

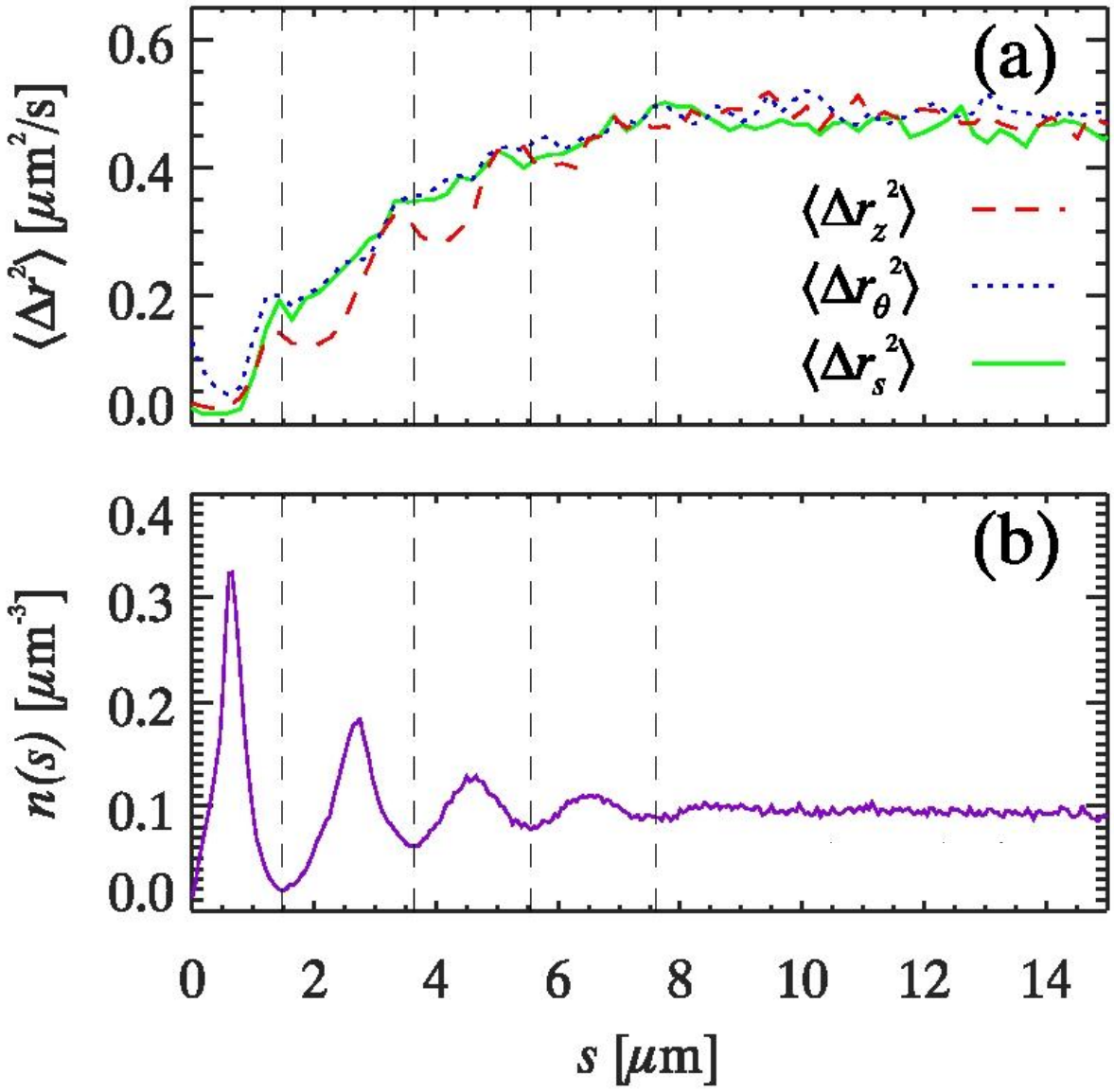

Figure 2.10: (a) Radial (r_s), angular(r_θ), and axial(r_z) components of mean square displacement (MSD) plotted as a function of distance from the center of the tube to the boundary of confinement; The radius of the tube is 19.8μm and ϕ= 51.4%. (b) Number density, n(r), plotted as a function of distance from the center of the tube to the boundary of confinement. The vertical lines correspond to the local minima of the number density, and the spacing between the vertical lines is about 2.3μm.

increase in a similar fashion as you move away the wall of confinement. The green and blue lines represent the radial and angular components of MSD respectively, and they both line up well. There are no significant peaks or dips in these forms of mobility, which means that the particles are able to easily move away from and towards the boundary and with a layer of

particle in the angular direction inside a large tube as this. The red line represents the axial MSD and is slower than the other two components and also shows more distinct jumps than the other two components. This means that the particles are moving slower when they are moving within and along a layer of particles inside the cylinder.

This reduced axial mobility is more pronounced and shows clear dips the closer you get to the walls and is a result of the layering of particles in that region. It is interesting to note that the peaks in $n(r)$ in figure 2.10(b) suggest layers of particles that correspond directly to dips in axial mobility for the particles in figure 2.10(a). As you move closer to the boundary, the layers become more distinct with the $n(r)$ showing sharper peaks, and the particles show a marked increase in mobility at those peaks. When you look at this phenomenon from a particle's point of view, a particle is moving along the wall and suddenly finds itself within a layer. The particle is content and does not have the desire to leave the comforts of residing in a layer. This is what causes a drop in axial mobility for the particles because they like to move within layers. Figure 2.11 shows the cross-section of the cylinder, and the particles are seen to reside in distinct layers. The layers are especially prominent closer to the walls and become less clear as you move closer to the center of the tube, which is confirming the ideas about reduced mobility due to layering near the boundary.

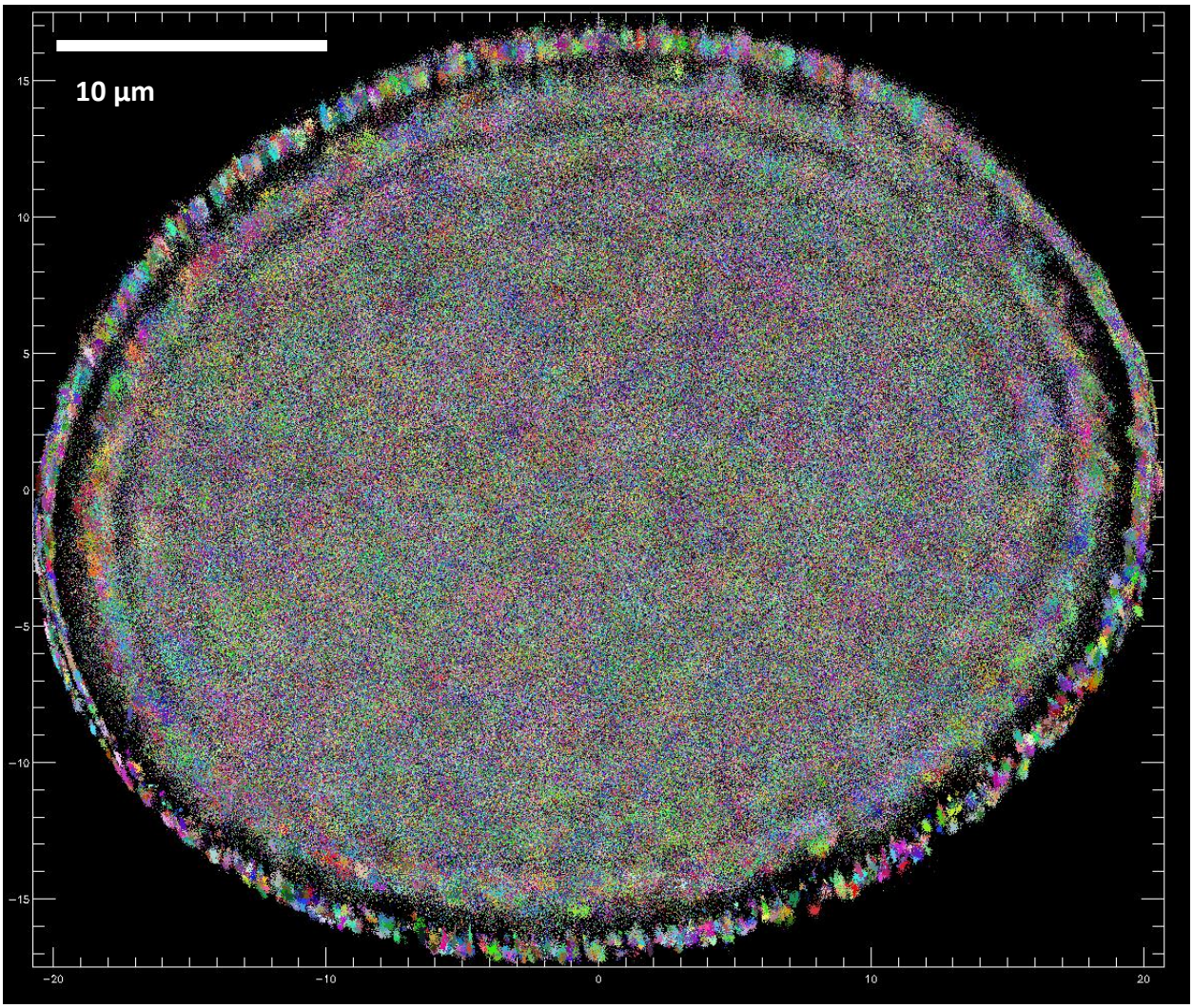

Figure 2.11: Cross-section of tube, layering of particles inside the tube along the walls. The radius of the tube is 19.8µm and ϕ= 51.4%.

Fig. 2.12 is a replica of Fig. 2.10, but the data is from a much smaller tube of radius 7.09 µm. Figure 2.12 (a) plots the MSD components of colloidal particles in the smaller tube, and they all speed up as you move away from the boundary, but unlike in the previous plot, there are distinct fluctuations in the mobility of particles in the cylinder for all MSD components as you their distance from the wall. The radial mobility is slower than the other two components, and the jumps in the green line for radial mobility are more pronounced than in the other lines, which suggest that the particles find it difficult to move away from and towards the wall. The

visible fluctuations in the axial and radial components suggest that the smaller radius of the tube causes mobility both within the layers and between layers to become challenging as between layers because they like to stay in layers for the most part.

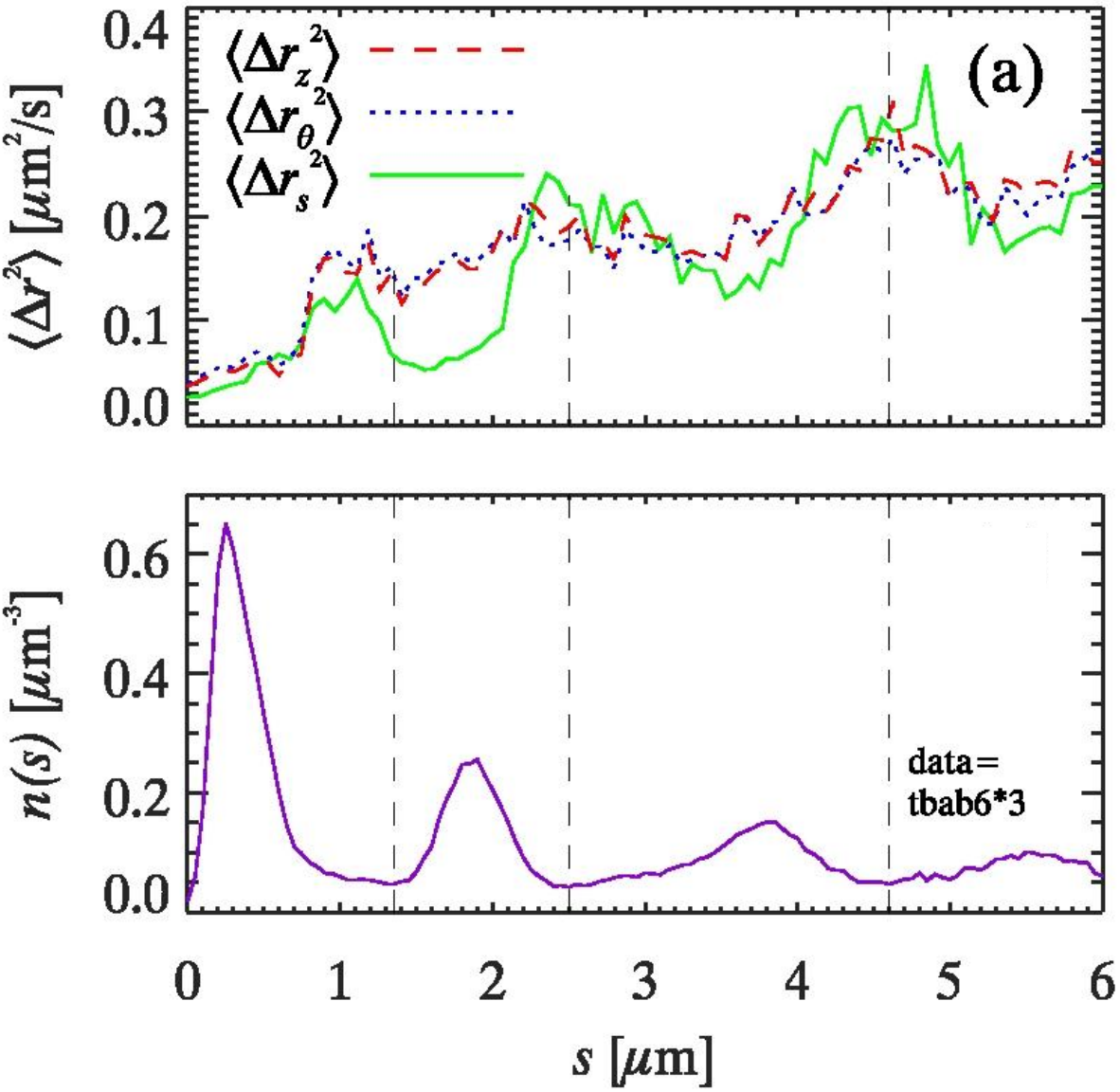

Figure 2.12: (a) Radial (r_s), angular(r_θ), and axial(r_z) components of mean square displacement (MSD) plotted as a function of distance from the center of the tube to the boundary of confinement. The radius of the tube is 7.09μm and ϕ= 43%. (b) Number density, n(s), plotted as a function of distance from the center of the tube to the boundary of confinement.

The layering of particles is much more pronounced in a smaller tube, as shown in Fig. 2.13, and this shows that a smaller confined cylinder makes it much harder for the particles to move overall. Perhaps the size of the tube influences the curvature of the walls, and the increased curvature affects how the particles are moving.

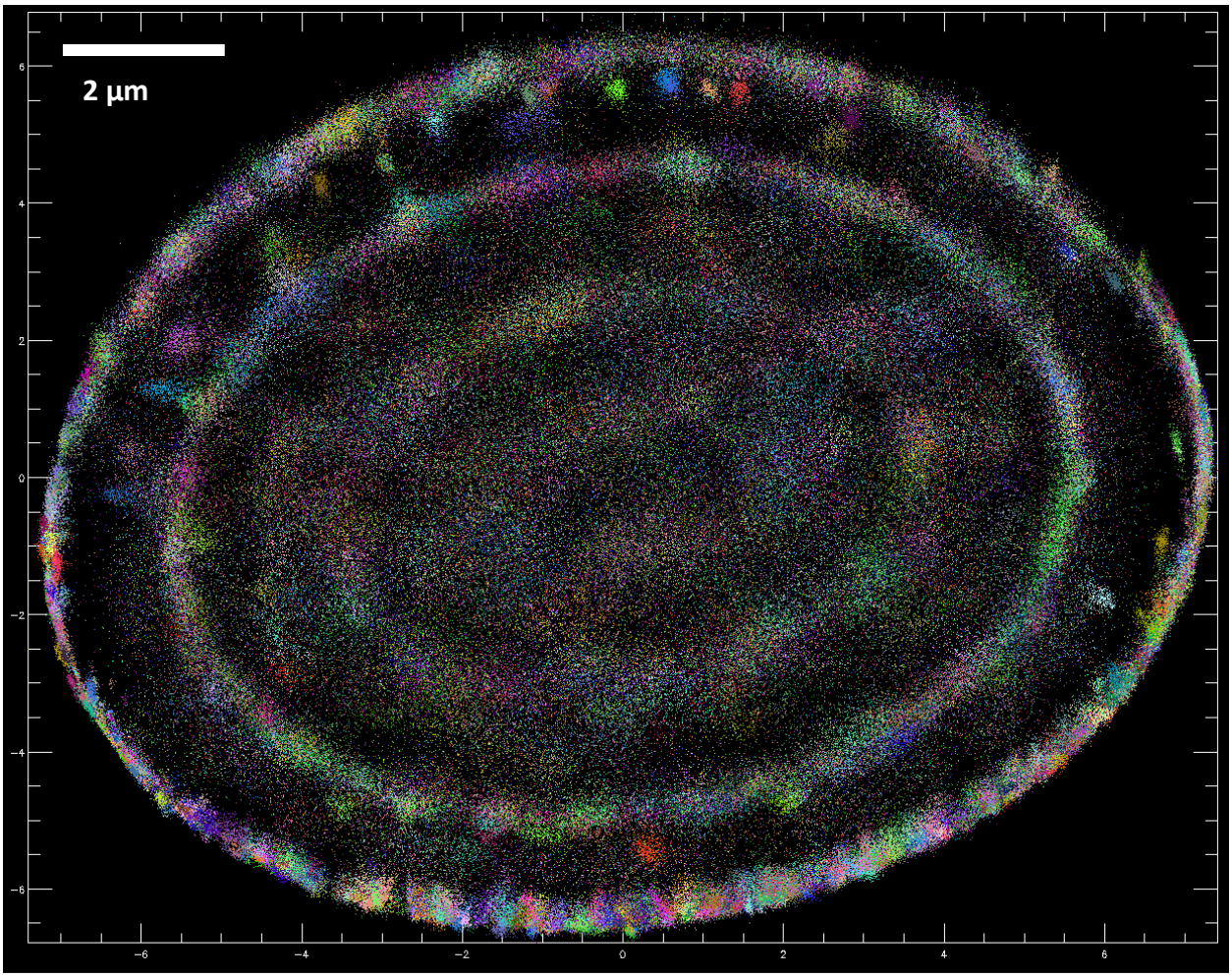

Figure: 2.13: Cross-section of tube, layering of particles inside the tube along the walls. The radius of the tube is 7.09µm and ϕ= 43%.

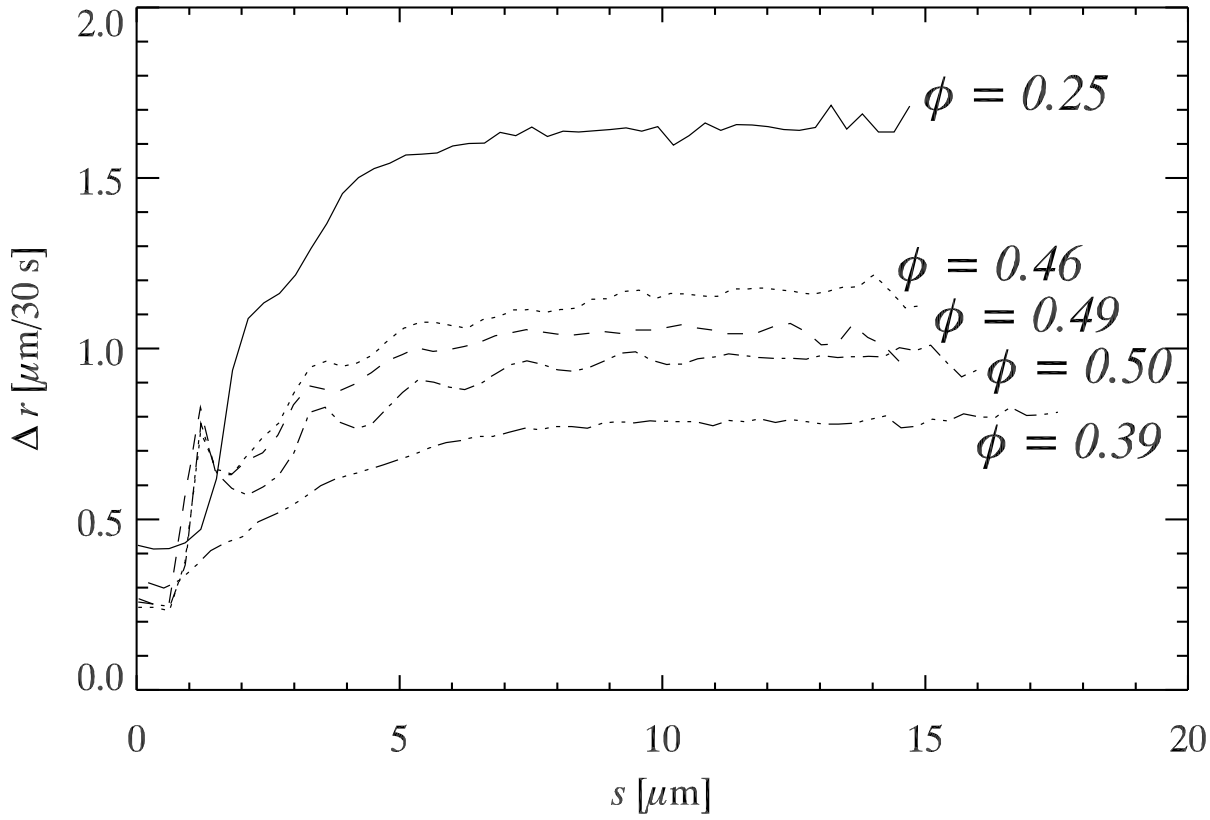

Figure 2.14: Mobility gradients from five different data sets with similar tube radii (R = 16.4±1.0μm). The y axis plots the average mobility for a 30 second lag time. The volume fractions from top to bottom are 0.25, 0.46, 0.49, 0.50, and 0.39.

So we can now move on to looking at the average mobility of different samples on the same plot in more depth and with respect to the distance from the wall. Fig. 2.14 is plotting the average mobility as a function of distance from the wall in order to understand better how the overall mobility changes with density of the sample. The data shown in Fig. 2.14 comes from a series of datasets with a much lower density and as you move from the top to the bottom in the series of lines in Fig. 2.14, the ϕ of the samples is increasing except for the very bottom curve with ϕ of 0.39. As you move along the lines from top to bottom, the curves are showing reduced mobility as the volume fraction increases each time. We can say that the plateau value is decreasing with increasing volume fraction ϕ and a constant radius. What this means is that as you confine the samples at higher volume fractions in the same radius, the particles are

slowing down correspondingly. However, the bottom line of ϕ= 0.39 shows that the experiment is not perfect, even though we are seeing strong trends in the data.

The volume fraction for the samples is calculated by counting the number of large particles in the cylinder, and it is likely that there is a large number of small particles in the φ= 0.39 data, and so the effective volume fraction is actually much larger than the calculated volume fraction. Also, different samples prepared from the same binary colloid may fill tubes differently depending on strain rates and other factors, meaning that even though the exact same colloids are used for an experiment, the volume fraction may be significantly different.

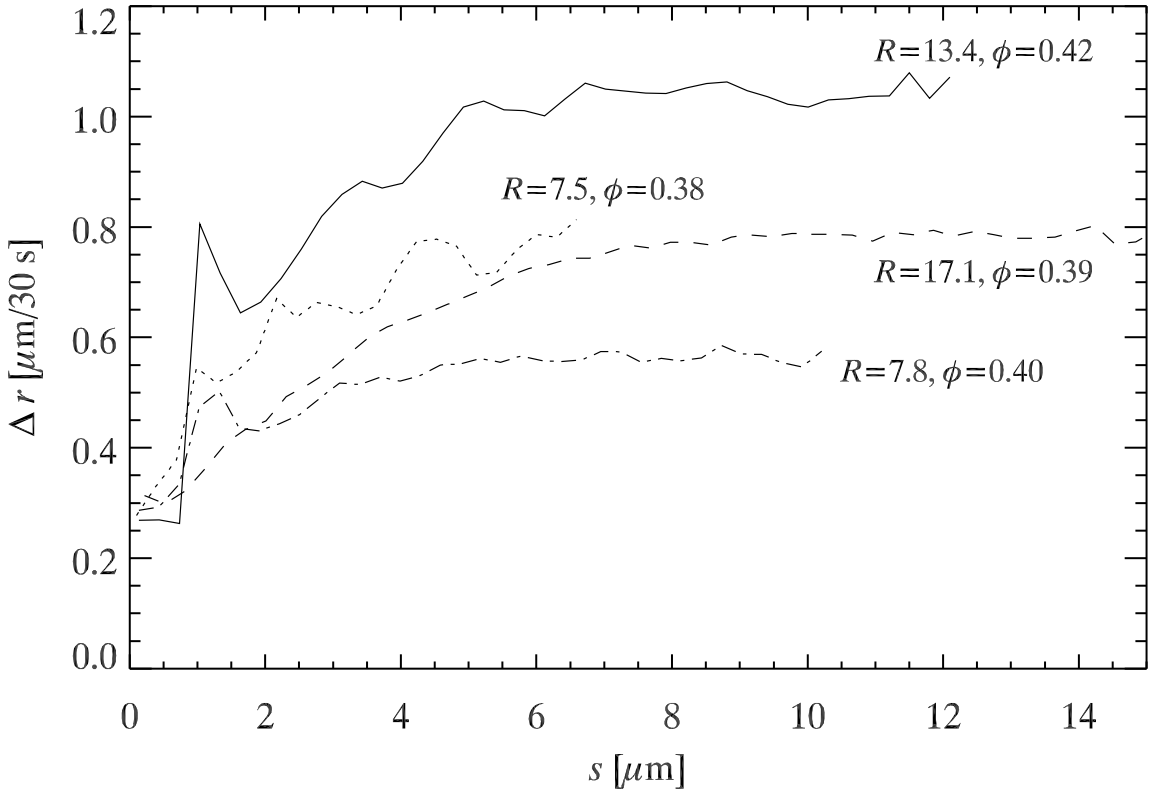

Figure 2.15: Mobility gradients from four different data sets with similar volume fractions (Φ = 0.396±0.020). The R values are 13.4μm, 7.5μm, 17.1μm and 7.8μm and their Φ's are 0.42, 0.38, 0.39, and 0.40 respectively.

We then want to see how the average mobility changes when you change the size of the cylinder. In Fig. 2.15, the four lines plot data with similar ϕ values and different tube radii. The

most striking feature of this figure is that there is no clear trend in the data at all. The data from the tubes of radii 7.5μm and 7.8μm have volume fractions of 0.38 and 0.40 respectively, so we would not expect the mobility to be too different, but in reality they are quite different. Also, the largest tube of 17.1μm has a slower mobility than the 7.5μm, which does not give us a clear picture of what confinement is doing to the particles.

Now that we have seen how moblity changes with layers, density and components in different samples, this is a good time to take a step back and think about why we are studying this one more time. The big picture question this thesis is trying to answer is "what does confinement do?" We want to know how the confinement effect actually changes what is happening inside the cylindrical geometry. The figures shown until this point paint an interesting yet unclear picture of the confinement effect, and we want to understand those ideas much better. We do this by fitting our data to a functional form to shed more light on the behavior of the data.

Studies have used functions to fit relaxation time (Scheidler, 2002), but we are interested in how mobility affects our system, and we are going to use mobilty as the the core of our argument. We want to understand the mobilty of the particles in three different ways, and we do so by using a function that has three fitting parameters that we can use for our data. We use the following function for this purpose:

$$\Delta r \approx C[1 - \beta \exp\left(-\frac{s}{\lambda}\right) \ ] \quad (2.3)$$

In equation above, s represents the distance from the boundary of confinement. The other parameters in the fuction explain different aspects of mobility. λ is a length scale and tells us how close you have to be from the confinement boundary for the particle to feel the effects of the boundary. C shows how fast particles are moving far away from the boundary, which is the bulk-like mobility for the sample. I will explain later how C seems to change with the radius of

the tube, which is why we can think of C as a plateau. β is a measure of how important of a role the confinement boundary plays in influencing mobility and has no units.

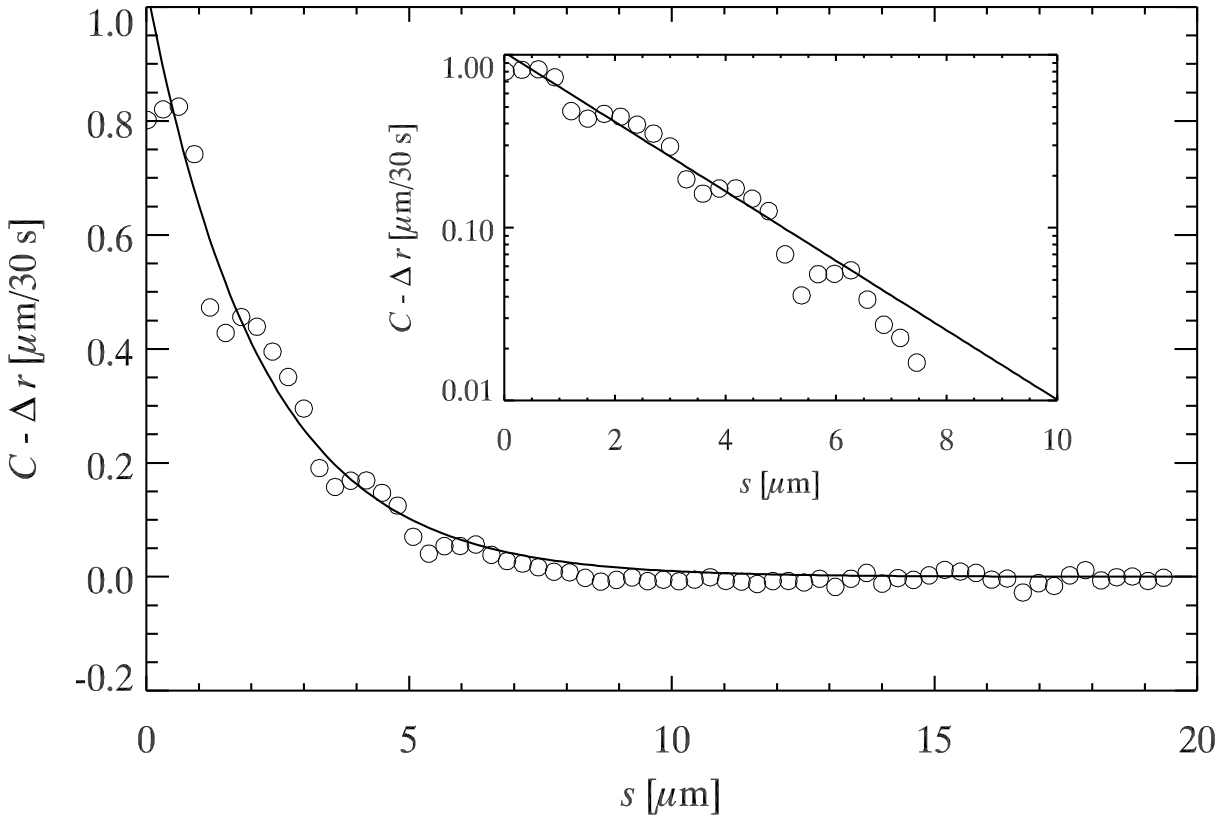

Figure 2.16: Exponential fit to mobility.This data corresponds to a cylinder of radius 20.91μm and ϕ of 0.51. Here the mobility has been subtracted from the plateau value C, and plotted lin-lin (main plot) and log-lin (inset). The circles are the mobility, the line is the fit using C=1.08μm, A=1.036μm, λ = 2.16μm.

We want to be able to fit the mobility of the particles as function of *s* using the formula in Eq. 2.3. Figure 2.16 simply shows that the mobility of the particles can be fitted to an exponential function on a lin-lin plot. Here the mobility has been subtracted from the plateau value C, and plotted on a lin-lin plot. We then replot the data on a log-lin plot as shown in the inset of Fig 2.16 and we can see that the fit seems to be working well, and the data looks like it has an exponental form. The decay length λ of 2.16 μm tells us how far away you have to go before the particles forget that there is a boundary nearby. Figure 2.1 6is simply trying to understand if

we can use the function in Eqn. 2.3 to fit our data, and the function seems to fit our data to suit our needs.

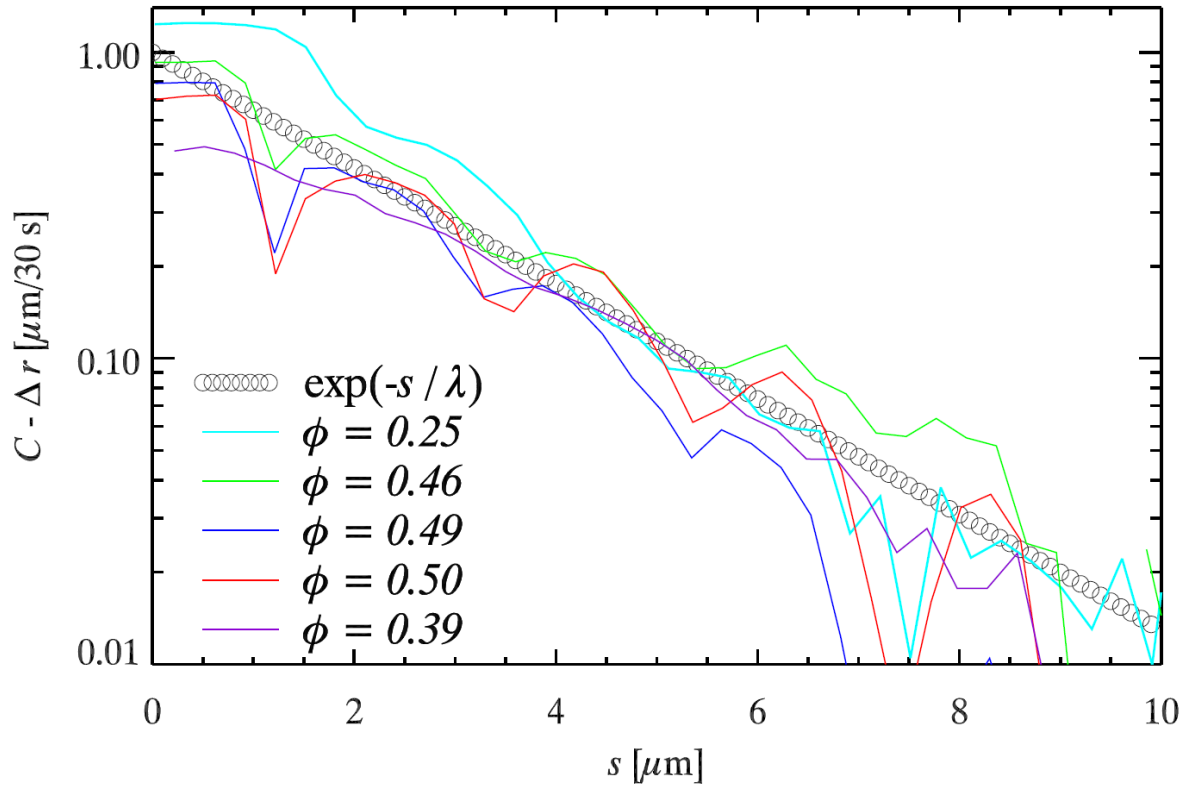

Figure 2.17: Plateau value C minus the mobilty plotted as a function of distance from the boundary of confinement for different values of phi as indicated in the legend.

Even though the function seems to be appropriate, more analysis is needed to draw significant conclusions from the data. Fig. 2.17 replots the data from Fig. 2.14 to show a different aspect of the information. Here the mobility has been subtracted from the plateau value C, and plotted on a semilog plot, so these should be straight lines if we are seeing exponential decay. For comparison, the black circles represent the exponential decay with a length of 2.3μm and was chosen to be close to the decay lengths determined by individual fits of the data. What this means is that we are seeing reasonably good fits to our data, even though it is not perfect by any measure.

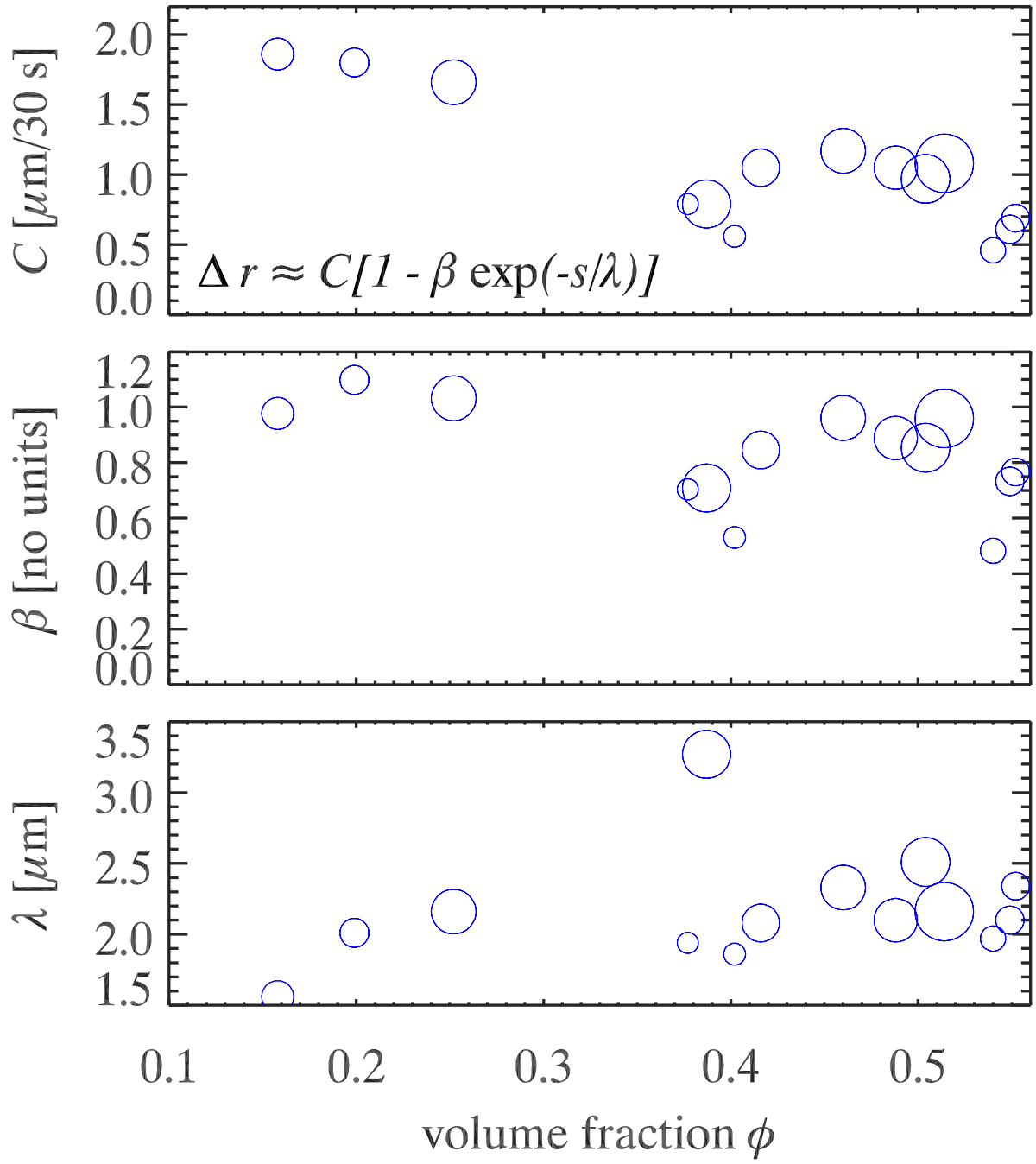

Figure 2.18: Values of the fitting constants plotted as a function of ϕ. The size of each circle is proportional to the tube radius, so the bigger circles represent bigger tubes.

Since we know that we can fit our data to Eqn. 2.3, we want to go ahead and plot the different parameters in the equation to see how they behave in our data. We do that in Figure 2.18 and

the circles' radii indicate the width of the tube the colloids are in, and the larger the circles on the plot, the bigger the tubes are. Fig. 2.18 at the top is plotting the plateau C as a function of volume fraction of large particles in the sample. As the volume fraction grows, the plateau C decreases, so that means that the particles are moving much slower even though they are far away from the boundary. C decreases with ϕ as we expect since C relates to the bulk MSD, which should get smaller as the tube gets smaller. In the middle plot of Fig. 2.18, β is somewhat decreasing with an increasing ϕ, which means that as the ϕ grows, the influence of the boundary on particle mobility decreases, which is a rather intriguing find. The length scale λ is at about 2.5μm, with perhaps a slight upturn as volume fraction is increased.

Fig. 2.19 plots the same parameters as Fig. 2.18, but plots them as a function of the tube radius to see if we can see something interesting happening. The size of the circles represent the volume fraction of the colloids, where a bigger circle represents a larger volume fraction. C is is not constant as fuction of tube radius and shows fluctions and a small upward trend. This behavior is unexpected, because C is supposed to measure the mobilty of particles far away from the boundary in a bulk sample, and should not depend on the tube radius at all. Since C changes as a function of tube radius, C can be best described as a plateau that is not really exhibiting bulk-like behavior. β increases slightly with the tube radius, so as the tube gets larger, the boundary might have larger influence on mobility of particles. λ decreases as the tube gets larger, so you have to be closer to the boundary for the particles to feel the effects of the boundary with larger tubes. However, all of these trends in the data are still up for discussion as we have yet to fully understand what all of this means.

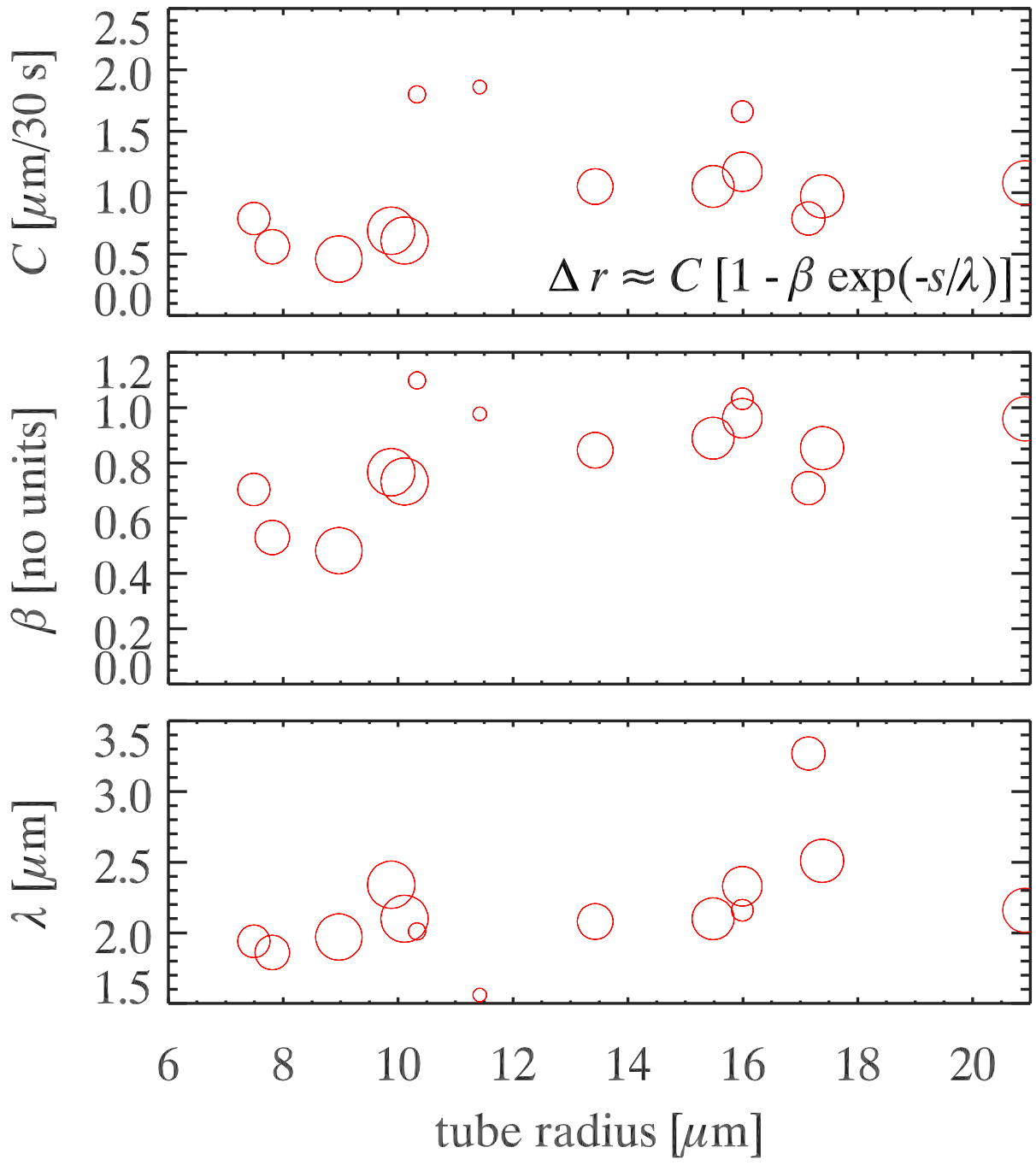

Figure 2.19: Values of the fitting constants, as a functio of R. The size of each circle is proportional to ϕ, so the bigger the size of the circle, the larger the ϕ value.

2.3 Conclusion

This experiment provided us with interesting ideas that we have not seen in previous studies on confinement. When we separated the MSD curves of different datasets into three components, all three components slowed down dramatically on getting closer to the boundary. In larger tubes, the radial and angular components line up well and the axial component was visibly slower overall and shows pronouced dips closer to the wall. The dips related to particles forming layers along the boundary, which also happened in smaller tubes. However, in the smaller tube, we saw the layers forming closer to the center of the tube, which greatly affected all three components of the MSD; in order for a particle to move a small step in any direction, many particles must reorganize within and between the closely packed layers, causing larger fluctuations in their MSD components, especially when the particles are moving between layers. This proves that confinement truly does change how glassy materials behave in interesting ways.

We then used an exponential fit to further characterize the mobility of the particles. We found that when the volume fraction grows, the "bulk" mobility decreases, the boundary becomes less important in affecting mobility, but the particles further away from the boundary feel the effects of confinement more. Examining how these parameters change with volume fraction revealed hints of trends: when we increased the volume fraction of the samples, the plateau value increased, the boundary had a more pronounced effect on the mobilty and the particles far away were feeling the effects of the boundary more. As the tube radius grows, the boundary becomes more important in affecting the overall mobility of particles and the particles must be closer to the boundary to feel its effects. However, the bulk mobility increases with the tube

radius, which was not expected, so we began to think of this parameter as a plateau instead of as the bulk.

This experiment did come with its fair share of challenges along the way. It was very difficult for us to confine samples of higher densities in small tubes, so we resorted to using lower volume fractions, which did eventually produce interesting results. The results from this cylindrical confinement experiment shed light on the complexities of the glass transition and make clear that understanding the behavior of glassy materials is not as simple as black or white, but there is plenty of gray in the story. We discovered that density of the confined samples, distance of the particles from the boundary and the radius of the confinement geometry all play important roles in determining glassiness in a system. All in all, we were successfully able to show that the dimensions of confinenment definitely affect how the particles behave in these spaces, which was the question we were trying to answer from the beginning.

Chapter 3

Decoupling of Rotational and Translational Diffusion in a 2D Granular Experiment

3.1 Experimental Details

Figure 3.1 shows the basic idea behind this experiment. I wanted to two-dimensionally study a cluster of three particles (also known as a trimer) in a sea of surrounding particles where the density of the neighboring particles could be altered at will. The choice of the tracer shape was

rather arbitrary, and mainly because we realized that this shape would be easier to track using IDL initially than other more complicated shapes such as hexamers, etc.

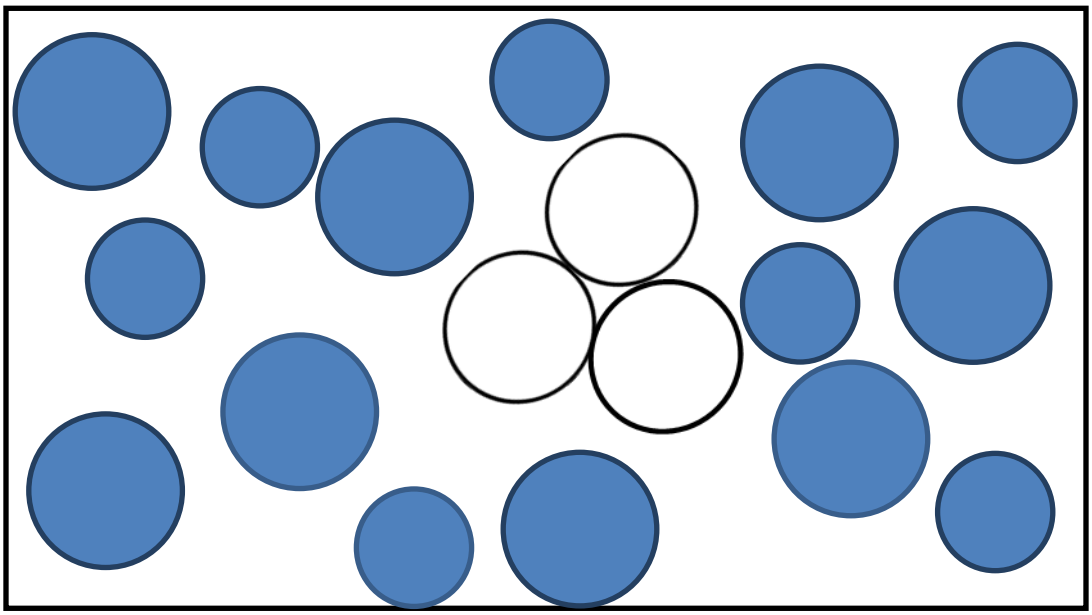

Figure 3.1: Diagram of the basic experimental idea.

This experiment is a 2D granular experiment that consists of macroscopic particles that are much larger than 1μm (so they are not affected by thermal fluctuations) and undergo a loss of energy when the particles collide. Granular systems are a good model system for us because we can induce a glass transition without having to change the temperature. A granular system can undergo a glass transition by simply changing the density of the system, like was done for colloids in the last chapter, and the amount of energy entering the system.

In this experiment, I used a shaker to input energy into a bed of particles and made them perform random motion in a 2D plane. The trimers I made for the system consisted of three delrin disks (made by McMaster-Carr) glued together as shown in figure 3.2. The black dots on the particles are for particle tracking purposes; as the particles are all white, the black dots contrast the background and can be identified by the software.

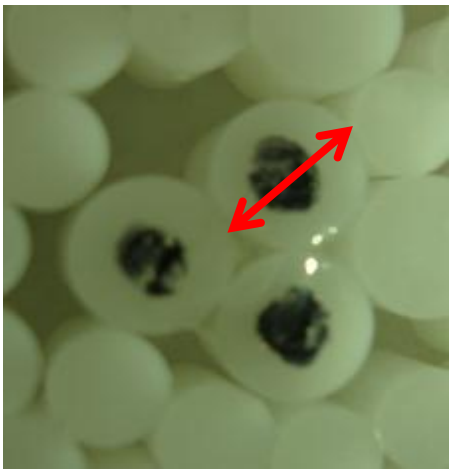

Figure 3.2: Image of a cluster of three delrin disks of diameter 0.64cm, as indicated by the red arrow, glued together to form a trimer. The trimer is surrounded by a bed of delrin disks of diameter 0.64cm and 0.56cm.

The trimer was place in a 15 cm-wide petri dish containing about 500 particles of two different sizes (0.64 cm and 0.56 cm). There are several steps that were taken to minimize the effects of crystallization because that would not accurately mimic the glass transition. This two-particle size system (also known as a binary system) and a size ratio of close to 1.5 (1.33 in this experiment) reduces the chances of the particles crystallizing (Desmond *et al.* 2009). The number ratio of small to large particles is also at 1.5, so at the highest area fraction of the system, there are 300 small particles and 200 large particles. This binary system is similar to the system used in the previous experiment in chapter 2.

Figure 3.3: Overhead view of large petri dish containing the trimer and surrounding particles. The dish is 15 cm wide.

I used a 14-inch loudspeaker to act as the shaker and had it connected to a function generator. The input was a regular sine wave from a function generator (Agilent 33220A 20 MHz Function/ Arbitrary Waveform Generator) and the maximum acceleration of the setup was 2*g,* with *g* being the acceleration due to gravity. The shaker was mounted on a three-legged platform, which enabled me to level the dish on the loudspeaker with a digital level as accurately as possible. It was important to level the dish to allow the particles to be spread out evenly across the dish and allow for more even shaking.

The dish was attached to the loudspeaker by a cork ring about 10 cm in diameter, with silly putty providing the adhesion between the cork ring and loudspeaker at the bottom and the cork ring and dish at the top. Silly putty was used because it had a sticky yet stable texture to it and was readily available. Other adhesive materials would have worked well for this purpose too.

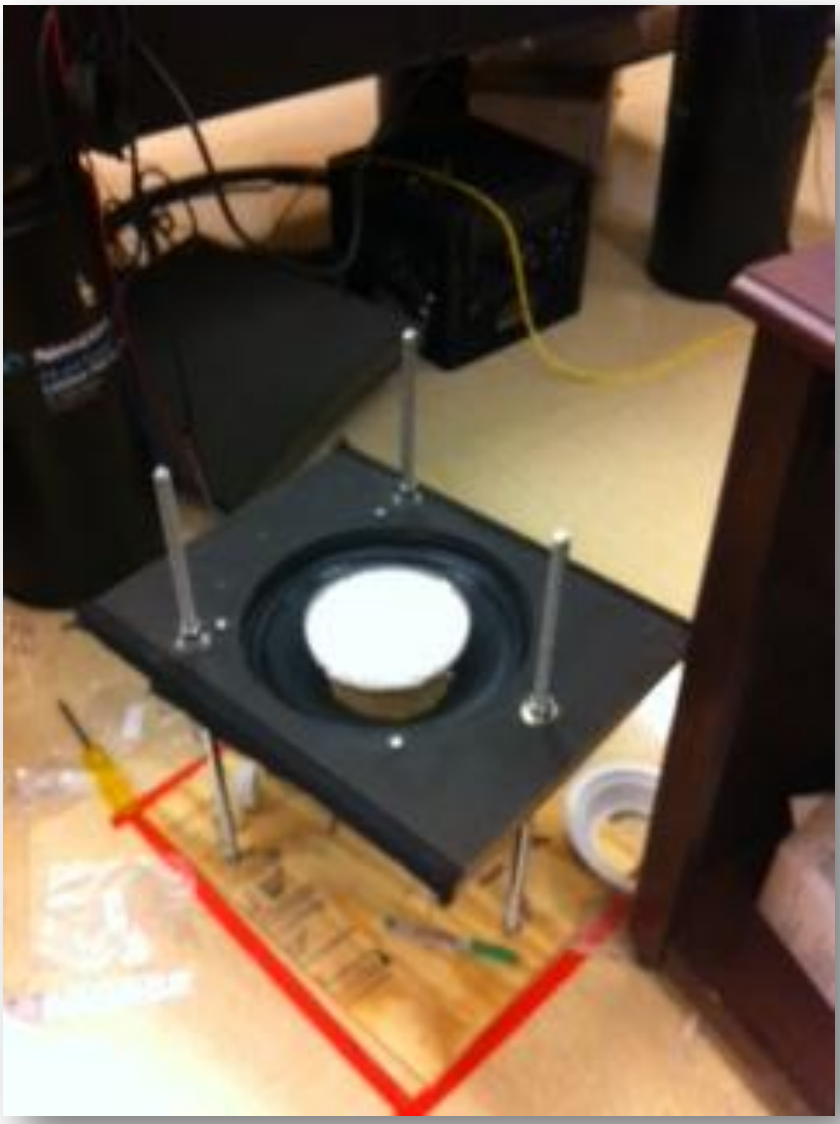

Figure 3.4: The experimental setup. The dish of particles is attached to the loudspeaker with a cork ring and silly putty. The loudspeaker is mounted on a custom made platform with 3 support stands to enable leveling of the system.

Data was acquired by mounting a camera (Panasonic Digital System Camera 5100) with a 60 mm lens (AF MICRO NIKKOR, 1:2.8 D) to a beam above the shaker system and the image series were saved as tiffstacks to a computer using Open Box software. Most datasets contained 2000 or 4000 images in a movie, and were taken at 3.3 frames per second, which

was fast enough that the particles could be tracked relatively easily using IDL and at the same time still allowed me to capture datasets over extended periods of time. The tiff datasets were then tracked using IDL tracking software with customized code to track particle clusters to extract their rotation and translation.

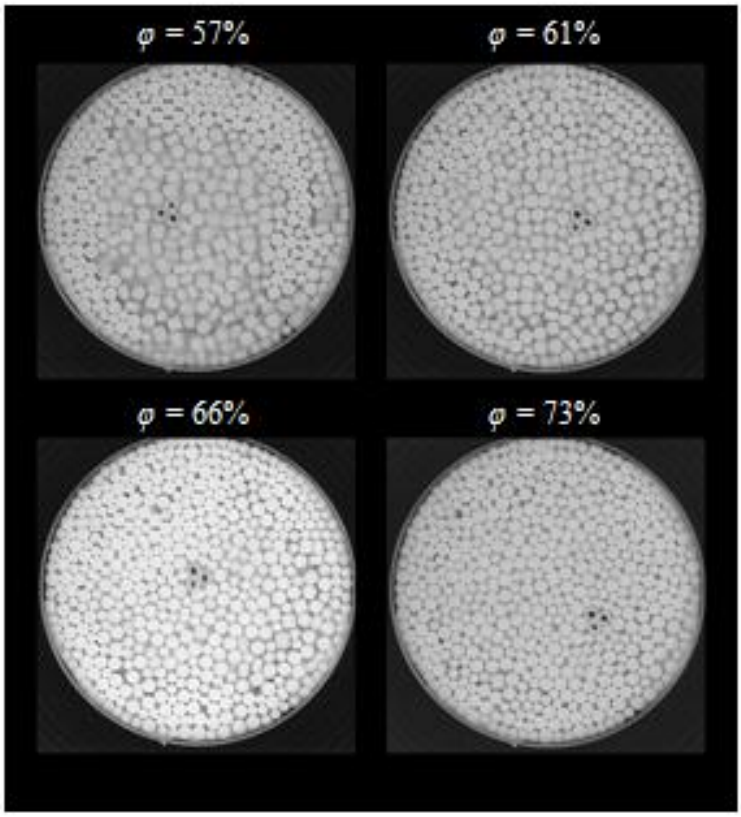

Figure 3.5: Images of datasets at four different area fractions φ.

The volume fractions used in Chapter 3 are accurate to a great extent because we control the exact number of particles that go into the dish for every experiment. However, since the dish is not being shaken uniformly throughout the entire region, the lower area fractions calculated are not exactly accurate, as there are pockets of more dense and less dense regions through the dish. Immobile particles tend to form a ring around the edge of the dish for lower area fractions starting at the calculated area fractions of around 58% or so. I looked at these individual

datasets and counted the number of particles in a small (5cm by 5cm) region area directly surrounding the cluster to check for the effective area fraction that is affecting the cluster. The effective area fraction directly surrounding the cluster at the lower range of calculated area fractions is quite different. A calculated area fraction of 57% seems to have an effective area fraction of about 38%, for example. However, since we have not yet started tracking all the particles surrounding a cluster, we cannot accurately determine the area fraction of particles directly influencing the cluster's mobility. But since this is a proof of principle experiment, I think we can allow for the area fraction to be a reasonable estimate. We are using the area fraction as an indicator of how many particles are in the dish to see how densly packed they are, so that will be enough information for us for our current purposes. However, in the future, every particle should be tracked in the dish and only the mobile particles surrounding a cluster should be used to calculate area fraction of the dish. The Table 3.1 shows some area fractions I counted the particles for in a 5cm by 5cm region around a cluster.

Table 3.1: Calculated and effective area fractions for datasets.

Data name	Calculated area fraction	Effective area fraction
13_2	0.57	0.38
13_3	0.57	0.34
13_4	0.57	0.34
11_1	0.60	0.44
11_2	0.60	0.50
11_3	0.60	0.45
11_4	0.60	0.47
10_1	0.61	0.46
10_2	0.61	0.44

3.2 Results

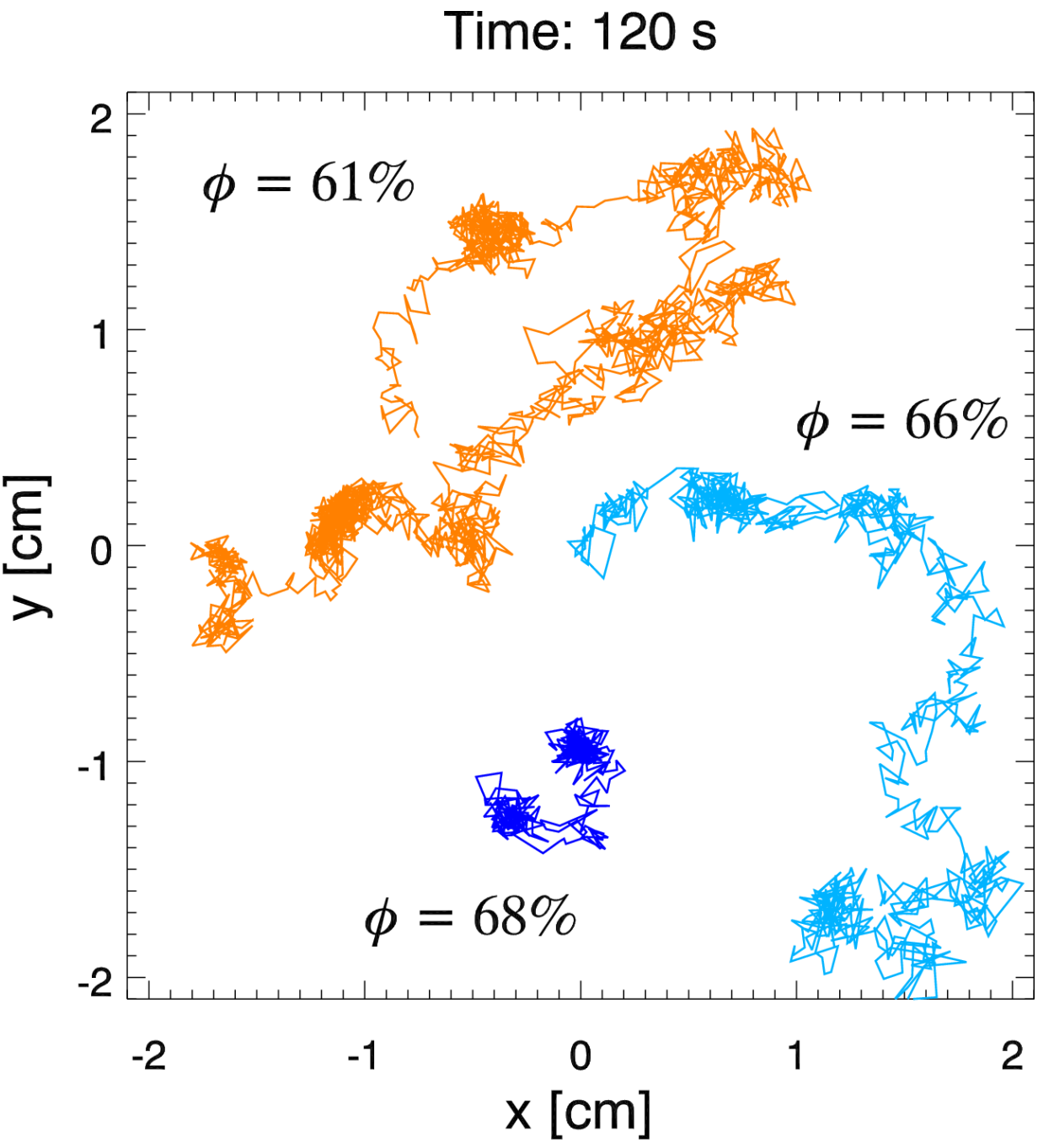

Figure 3.6: Trajectories of the center of mass for trimer at different area fractions showing cage breaks.

Each trimer's center of mass can be tracked to produce trajectories as the ones shown in Fig. 3.6, which shows the particle trajectory for the trimer diffusing in three different area fractions. The densest sample ($\varphi = 68\%$) shows the most limited mobility as the particle seems to be restricted to moving around in a small region. When you look more closely at the trimer trajectory, you see that the trajectory maps out into two distinct clumps. This phenomenon can be described as "cage breaking" (Hunter and Weeks 2012). The cluster is initially trapped in a local cage and then jumps to a new spot due to cage rearrangements.

The cluster becomes "caged" (Schwiezer and Saltzman 2003; Weeks and Weitz 2002) as it gets trapped in a small area due to the surrounding particles. Often the wall of particles trapping a cluster starts moving a little bit and the cage-breaking particle moves with the wall. Then the wall starts moving because the particles around it start moving, and in order to move at all, all the particles have to move cooperatively. The cluster is able to make a jump to a neighboring open spot, which is called cage breaking. This idea can be thought of in terms of an energy landscape, where the cluster is caging around a local minimum and then relaxing over an energy barrier, leading to a cage break (Hunter and Weeks 2012).

The other two trimer trajectories in Fig. 3.6 are from a datasets with a lower area fraction, and the trimer is translating a greater distance in both cases. Close observation reveals the existence of cage breaks in these data sets as well, but perhaps not as pronounced as in really dense systems. As the area fraction of the system is decreased, the cage breaks become less obvious.

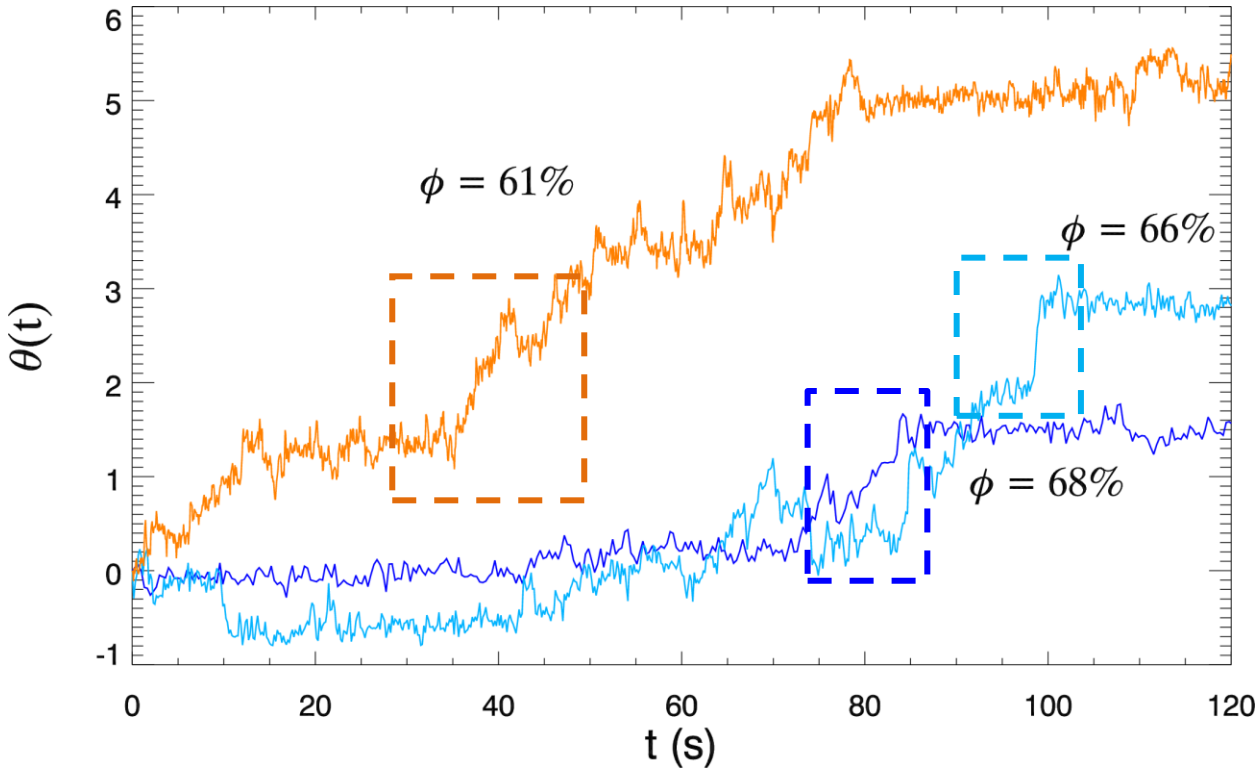

Figure 3.7: Angular trajectories of the clusters for trimer at different area fractions showing angular cage breaks. Dotted boxes indicate cage breaking.

We then wanted to look at whether or not a system is performing angular cage breaks or not. Fig. 3.7 plots the angular cage breaks in the system. The dark blue line shows the densest data set and you see one distinct cage jump in the indicated spot. The other two data sets are less dense and show angular cage jumps too.

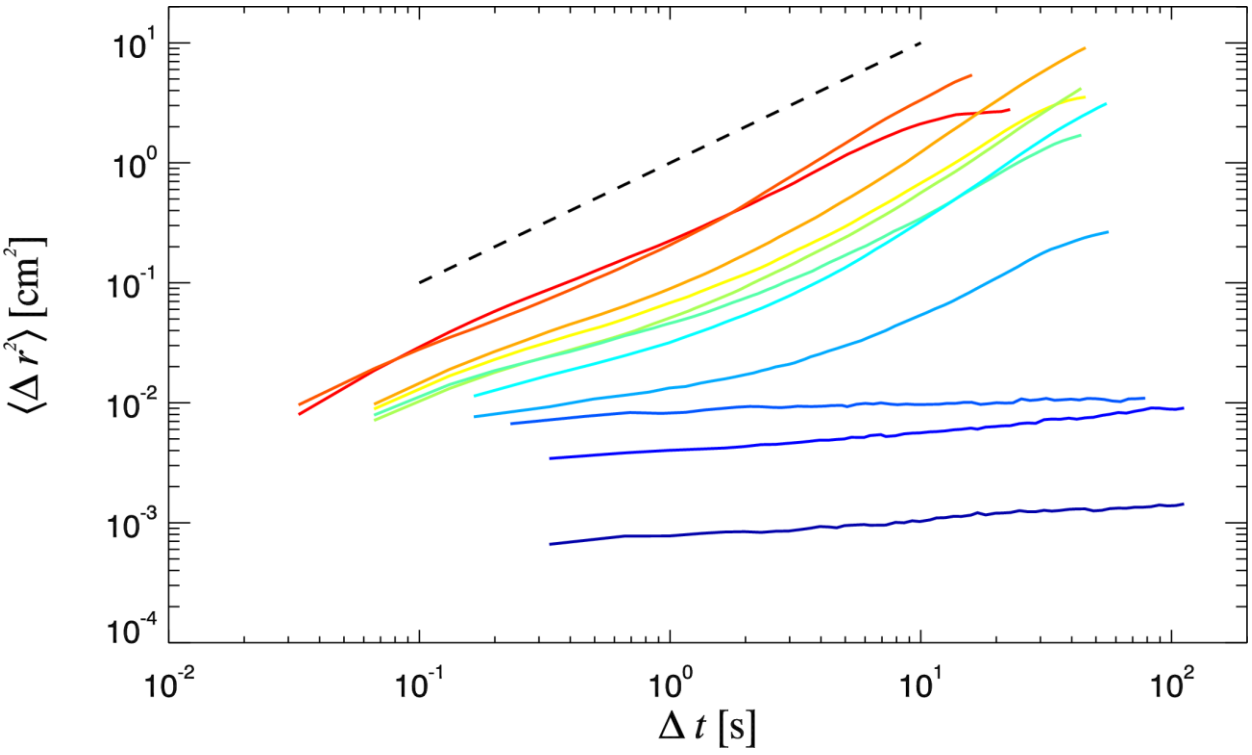

Figure 3.8: Mean-square displacement of a trimer in different φ's over lag time. Φ increases when going from red to blue in this order: 0.572, 0.581, 0.595, 0.614, 0.628, 0.636, 0.661, 0.680, 0.694, 0.713, and 0.727. The dotted line represents diffusive behavior.

The mean square displacement (MSD) curve plots the mobility of the trimer vs. lag time on a log-log plot. When an MSD has a slope of 1, as represented by the dotted line on Fig. 3.8, the particles are fully diffusive. Plots with a slope of less than 1 have subdiffusive particles. In Fig. 3.8, the red datasets have the lowest area fractions of 57% and the dark blue line has an area fraction of 73%. The area fraction φ is determined by dividing the total surface area of all the particles in the dish by the total area of the dish. It is clear the slope of the lines decreases dramatically as you go from the low area fractions (red) to higher area fractions (blue). The particles are undergoing somewhat of a glass transition as there is dramatic slowing down of particles are they become more closely packed together.

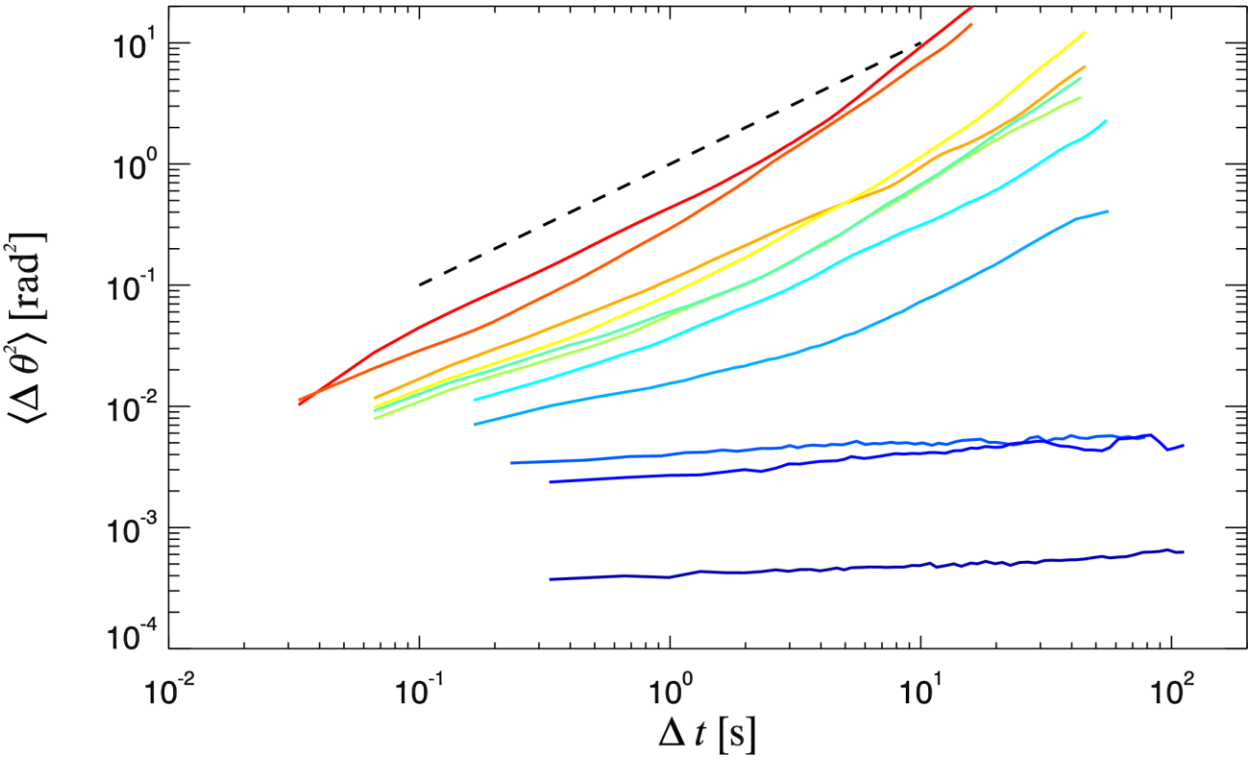

Figure 3.9: Mean-square angular displacement (MSAD) of a trimer in different φ's over lag time. Φ increases when going from red to blue in this order: 0.572, 0.581, 0.595, 0.605, 0.614, 0.628, 0.636, 0.646, 0.661, 0.680, 0.694, 0.713, and 0.727. The dotted line represents diffusive behavior.

The mean-square angular displacements (MSADs) plotted in Fig. 3.9 show a very similar trend to the MSDs, where a higher φ on approaching the glass transition reduces the angular mobility of the trimer. Now that we are able to extract the MSDs and MSADs from our data, the next step is to obtain the diffusion coefficients from the data and calculate the ratios of the translational and rotational diffusion.

I obtained the diffusion coefficient by fitting a line of slope 1 (which indicates regular Brownian motion) to a portion of the MSD or MSAD curve that looks like it has a slope of one. Once this fitted line is obtained, the point of intersection with the y axis of the straight fitted line is divided by 4 to obtain the translational diffusion coefficient D_{tr} and the same process applies for

the rotational diffusion coefficient D_R, but this value is divided by 2 instead of 4. The 48 fitting plots for both the MSDs and MSADs are show over the next several pages.

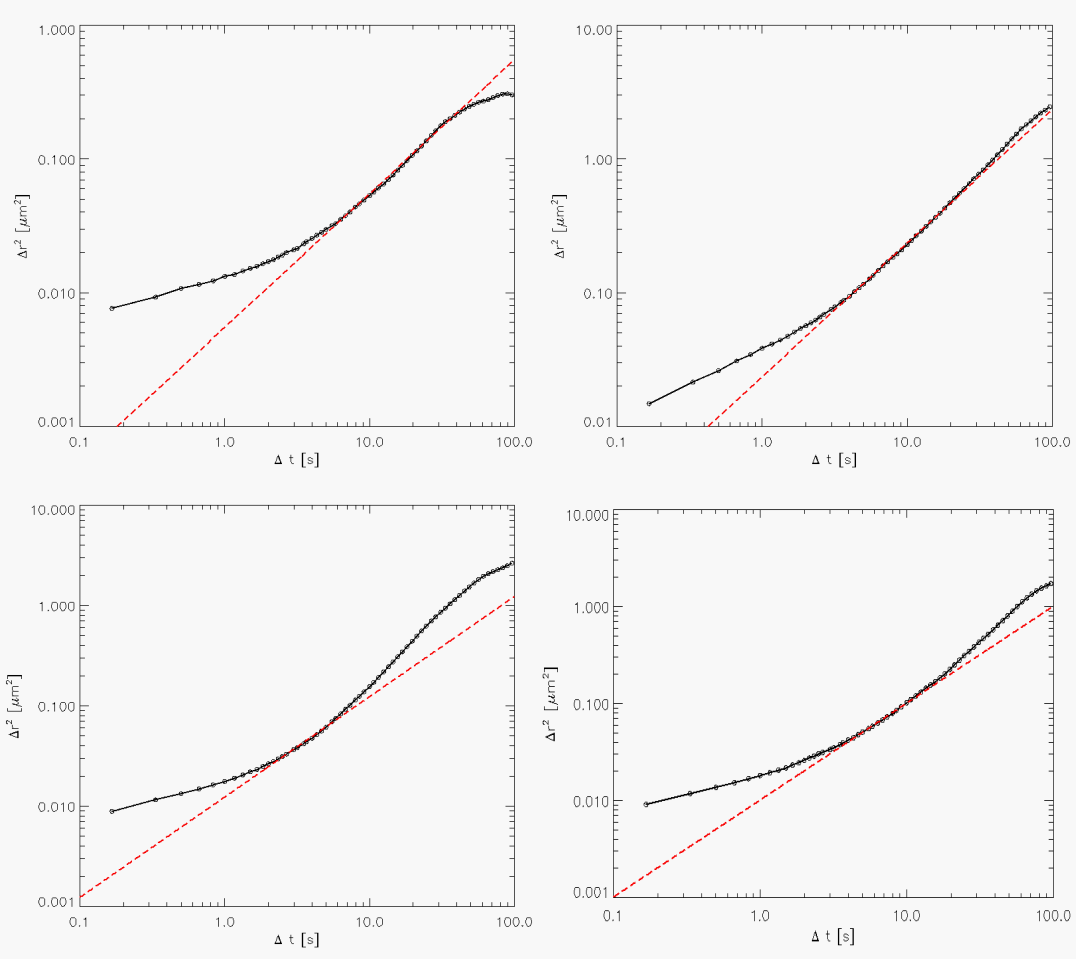

Figure 3.10: Fits made on the MSD plots with φ= 0.68.

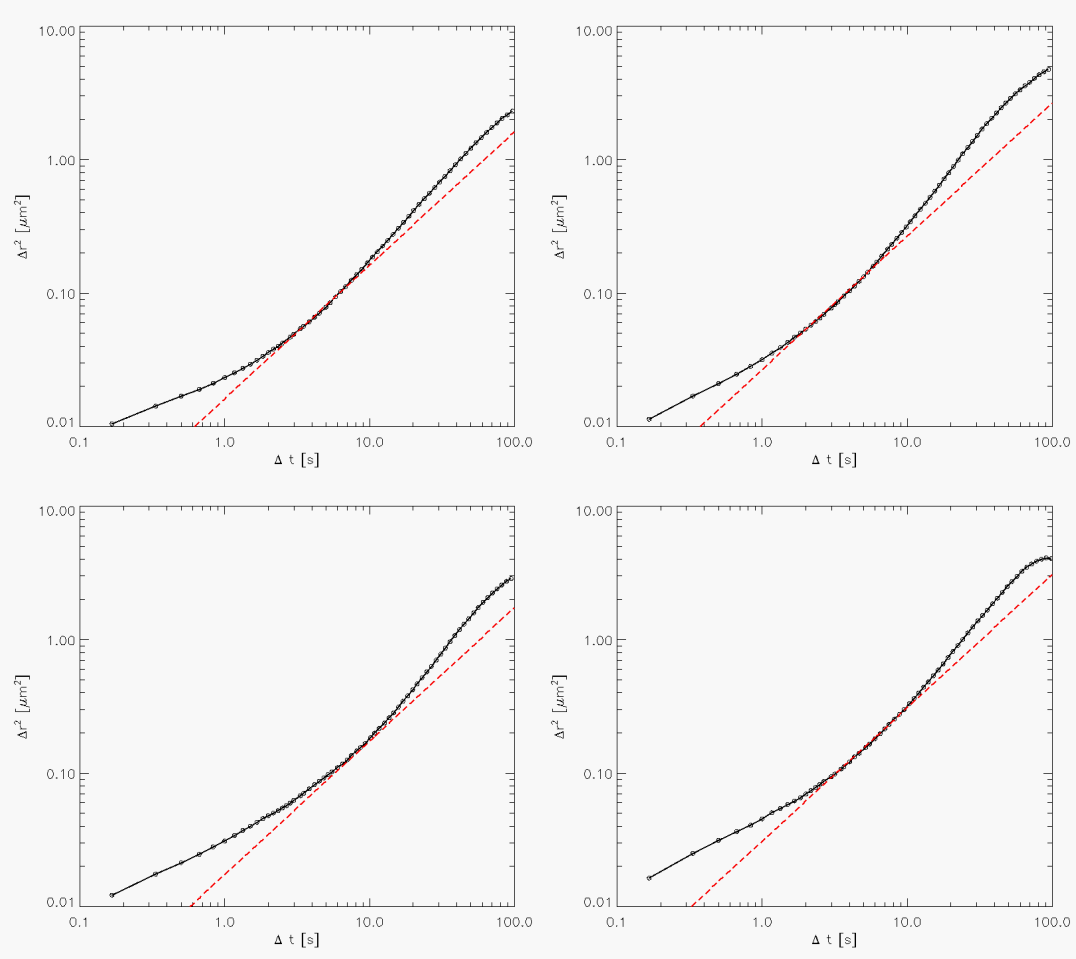

Figure 3.11: Fits made on the MSD plots with φ= 0.66.

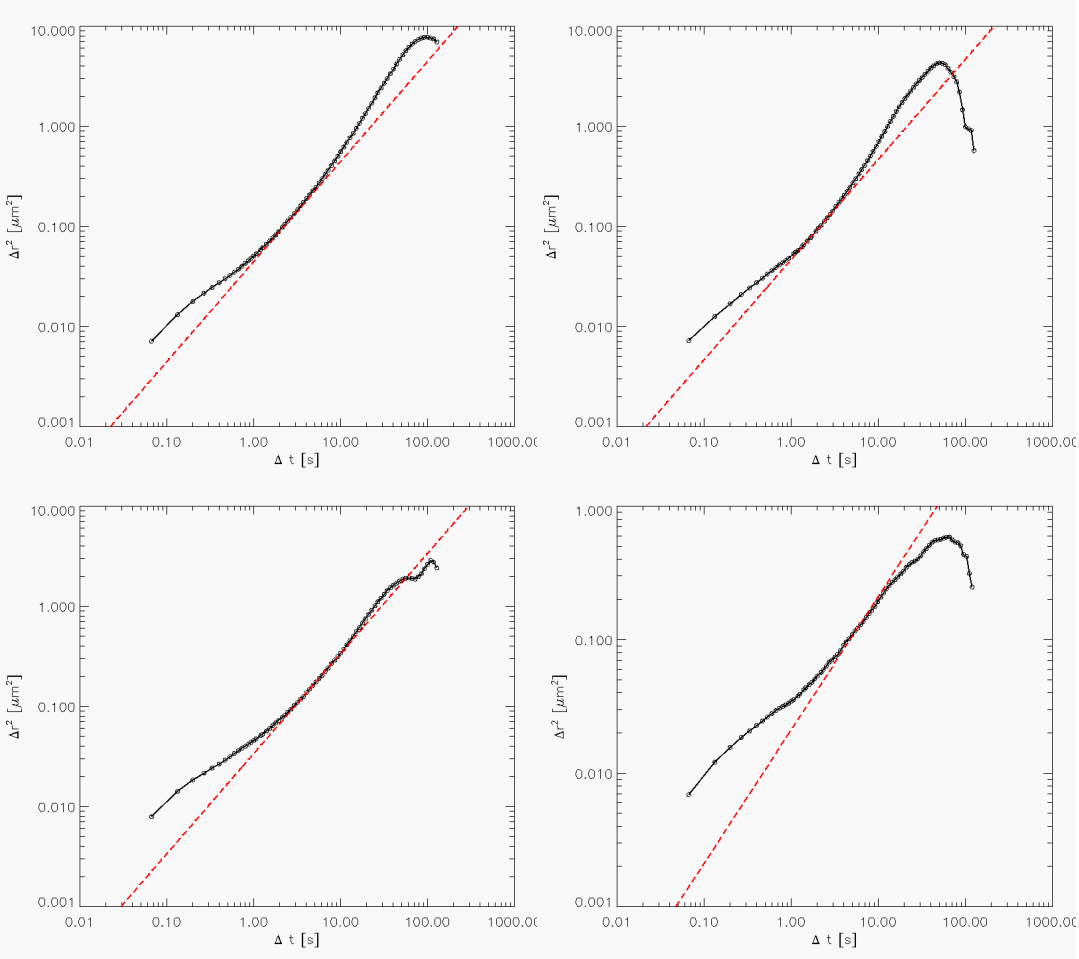

Figure 3.12: Fits made on the MSD plots with φ= 0.64.

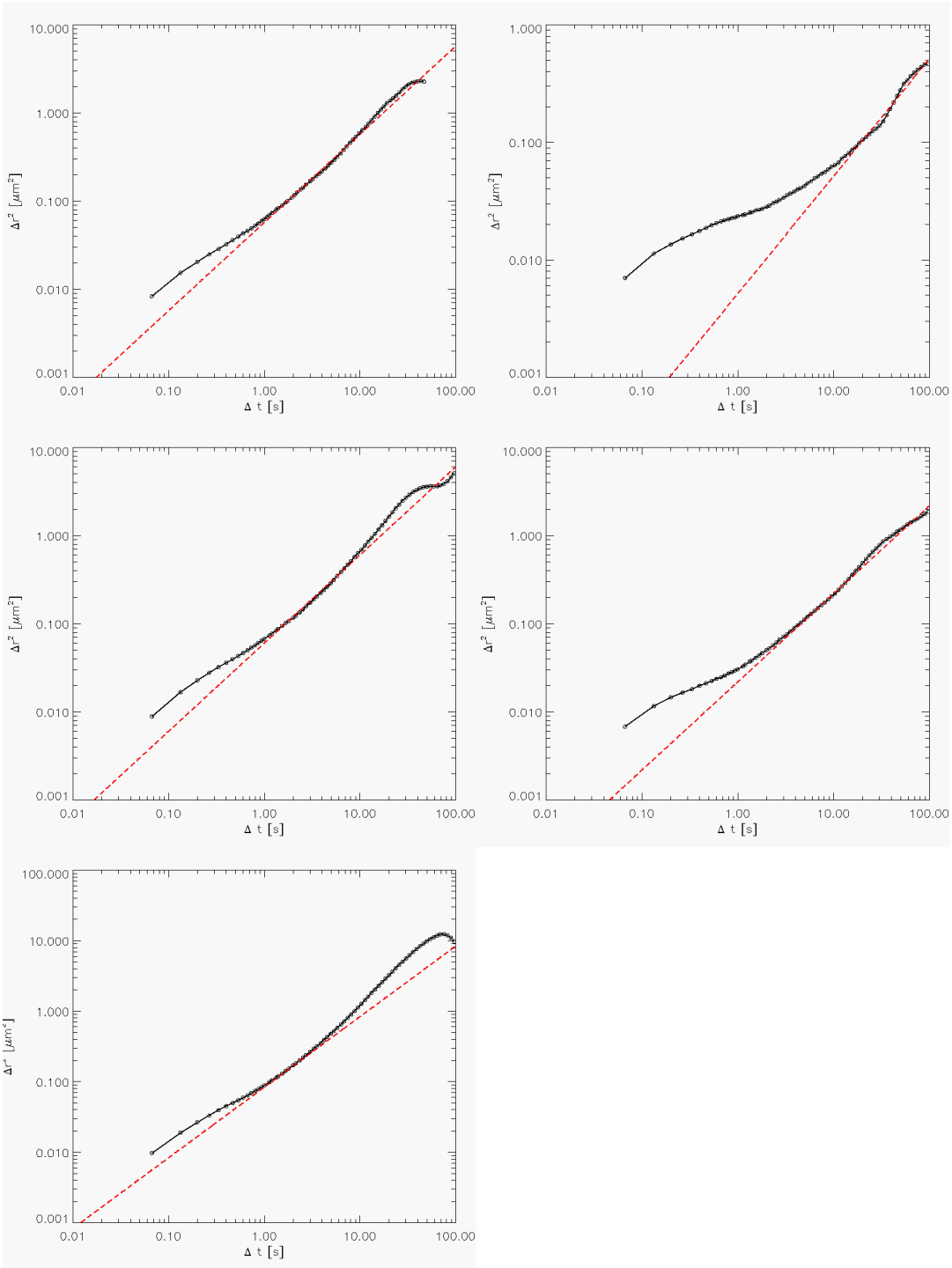

Figure 3.13: Fits made on the MSD plots with φ= 0.61.

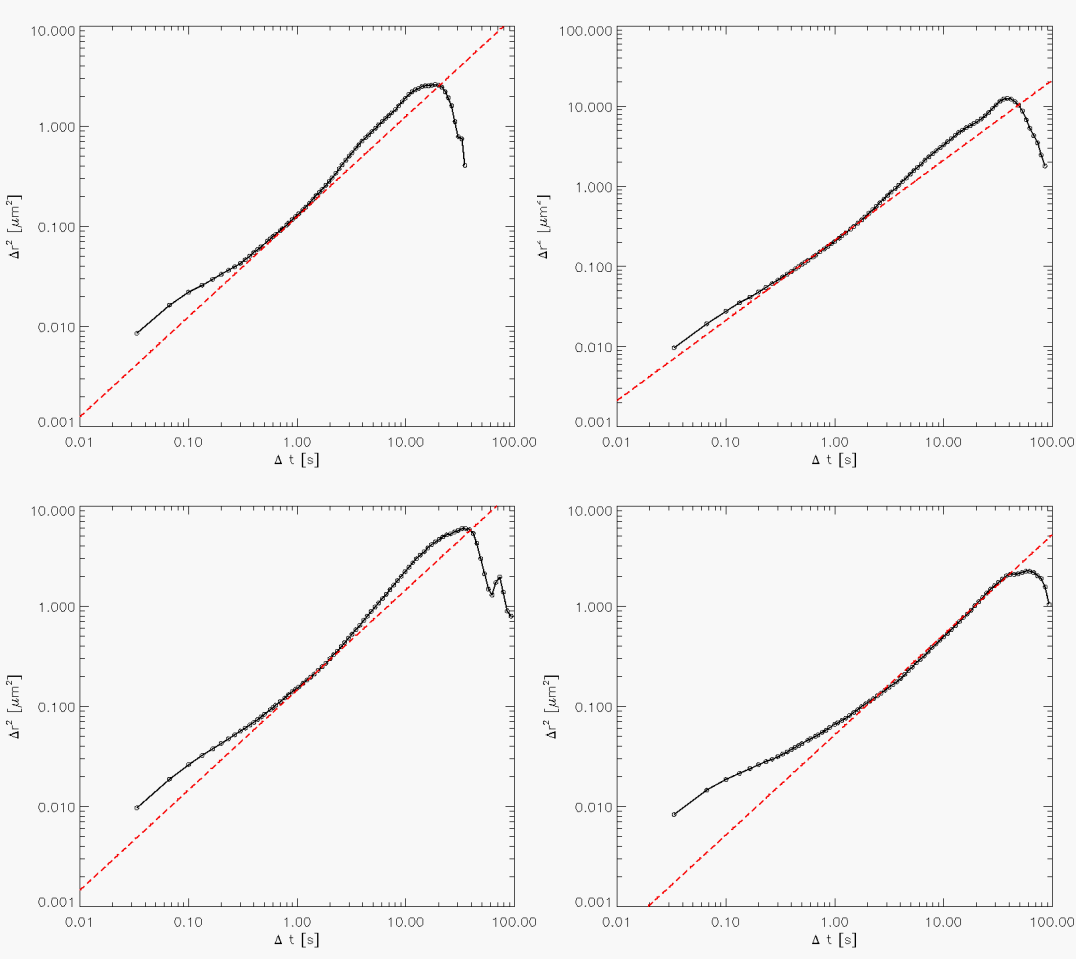

Figure 3.14: Fits made on the MSD plots with φ= 0.60.

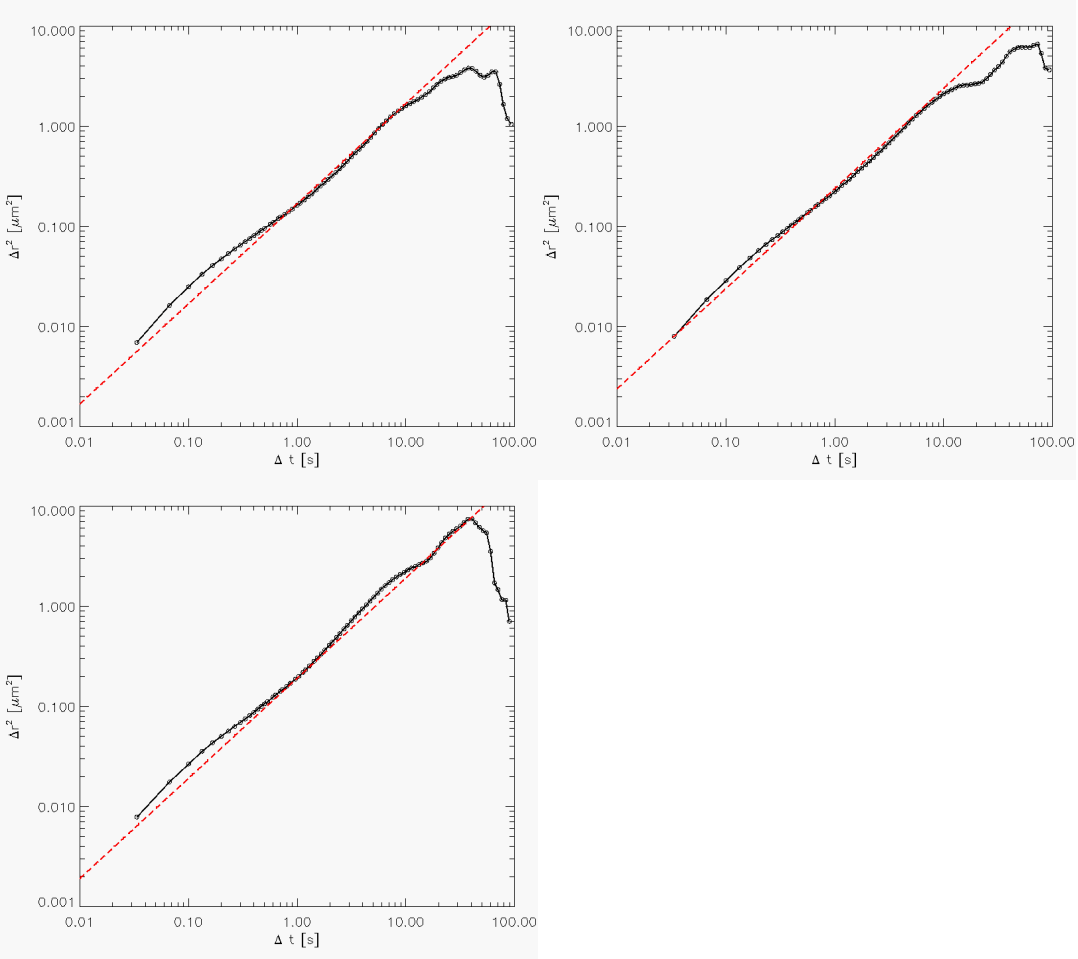

Figure 3.15: Fits made on the MSD plots with φ= 0.57.

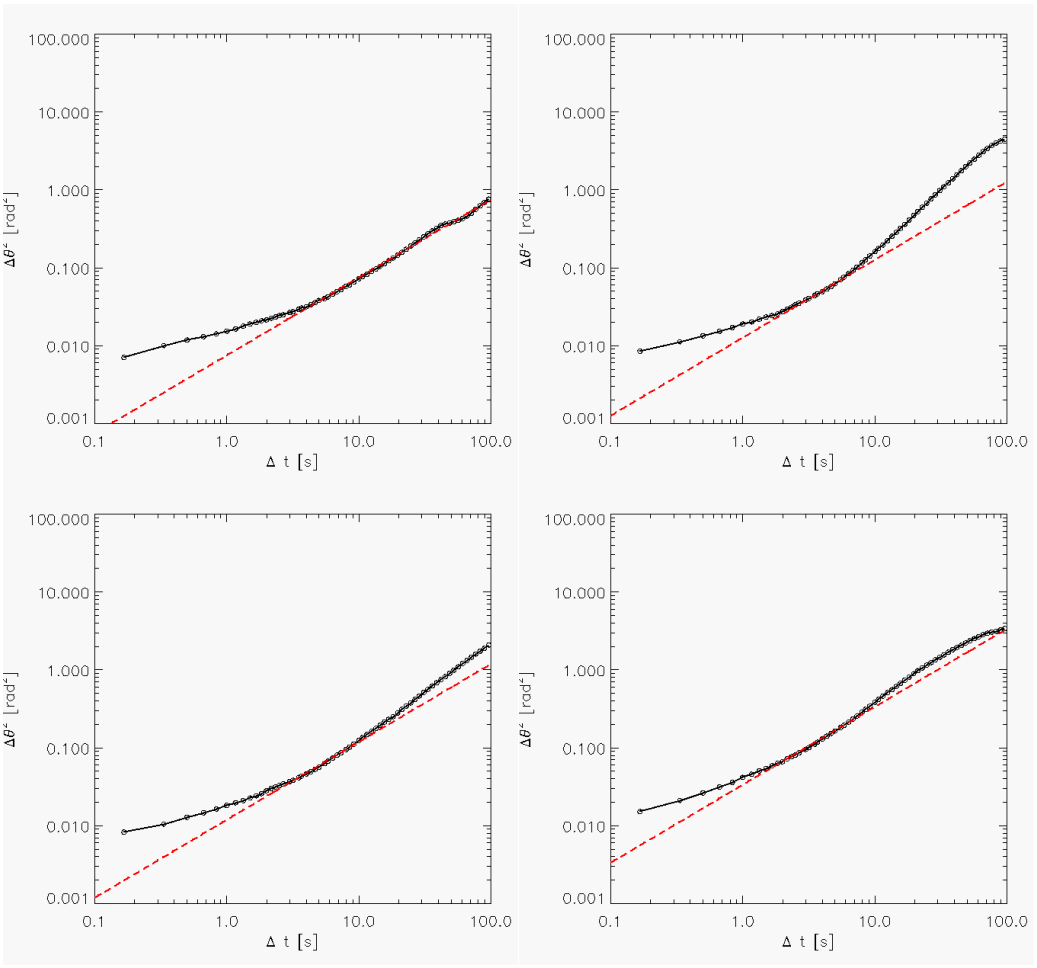

Figure 3.16: Fits made on the MSAD plots with φ= 0.68.

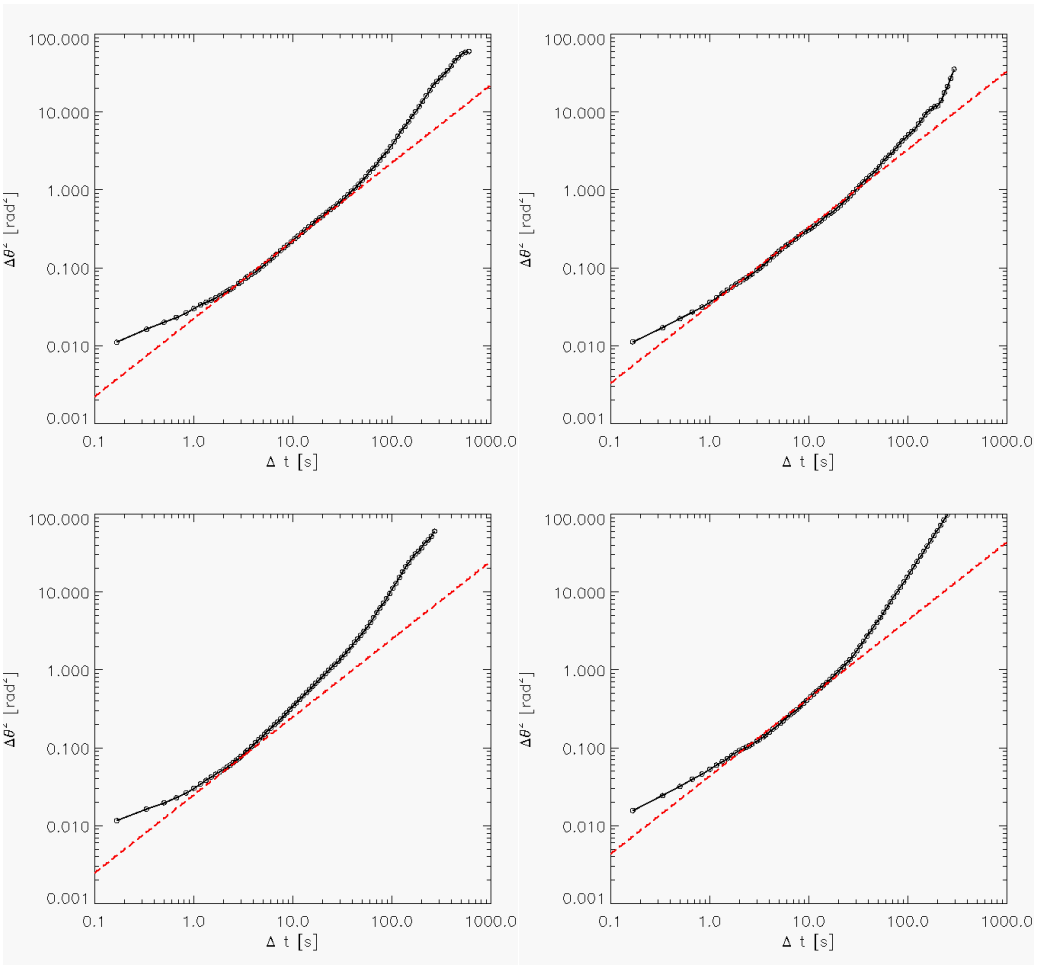

Figure 3.17: Fits made on the MSAD plots with φ= 0.66.

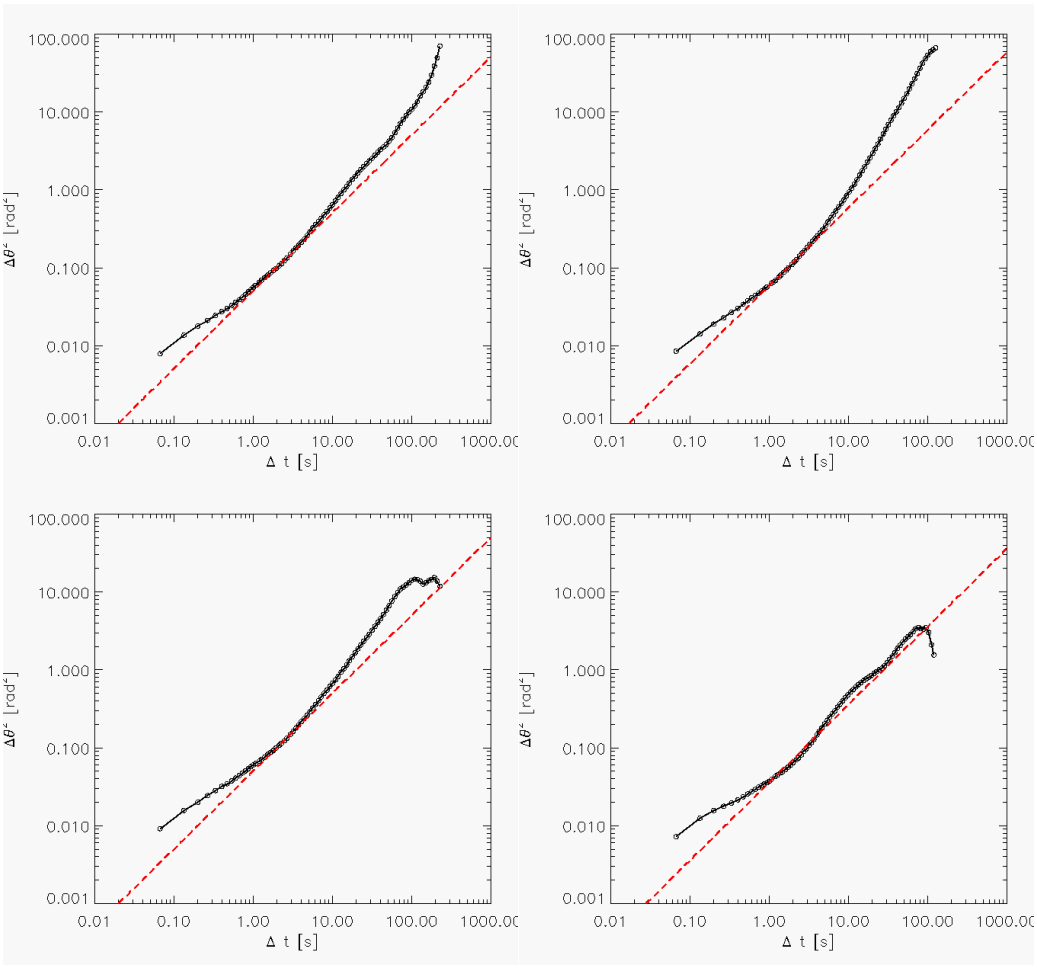

Figure 3.18: Fits made on the MSAD plots with φ= 0.64.

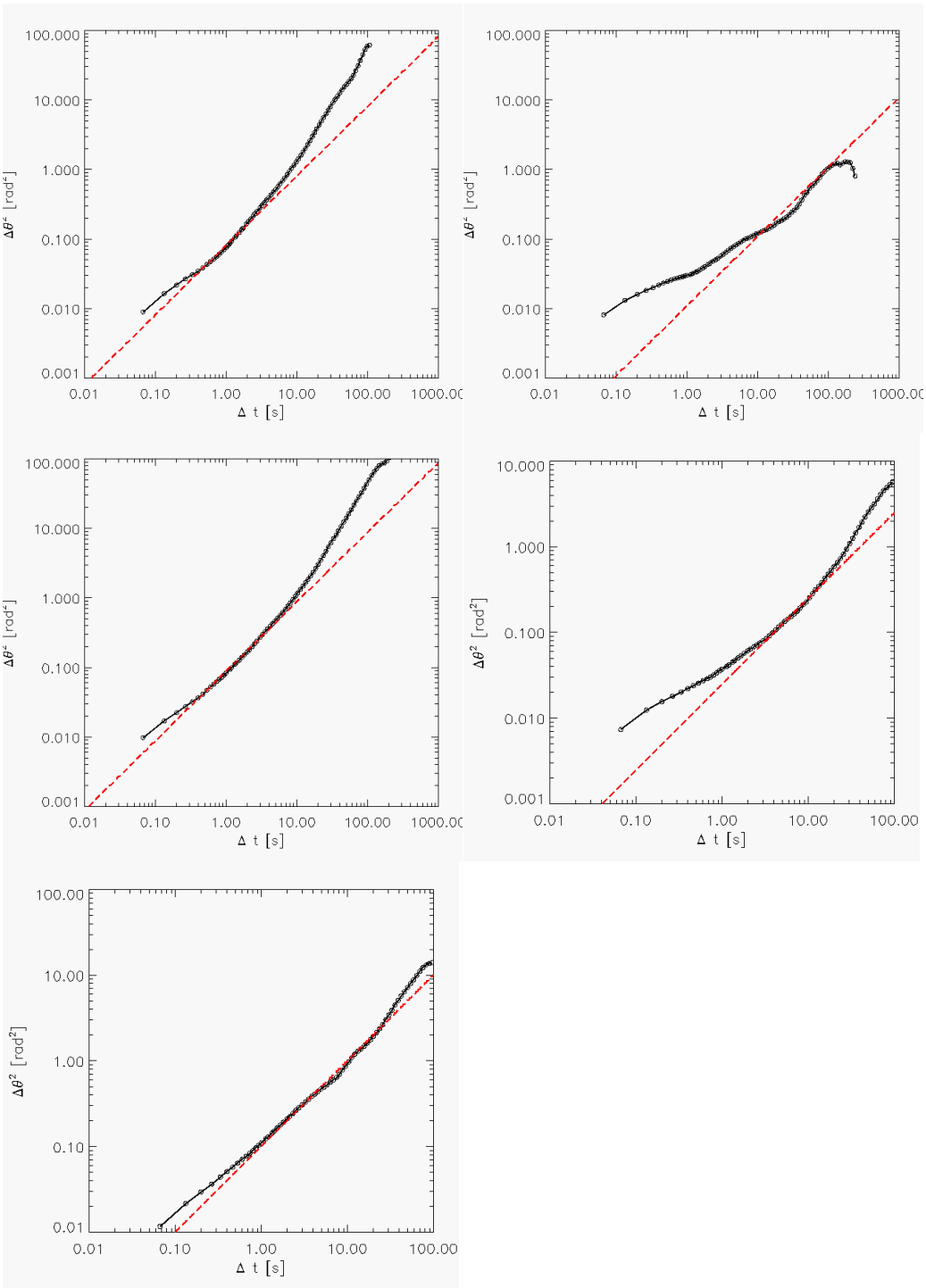

Figure 3.19: Fits made on the MSAD plots with φ= 0.61.

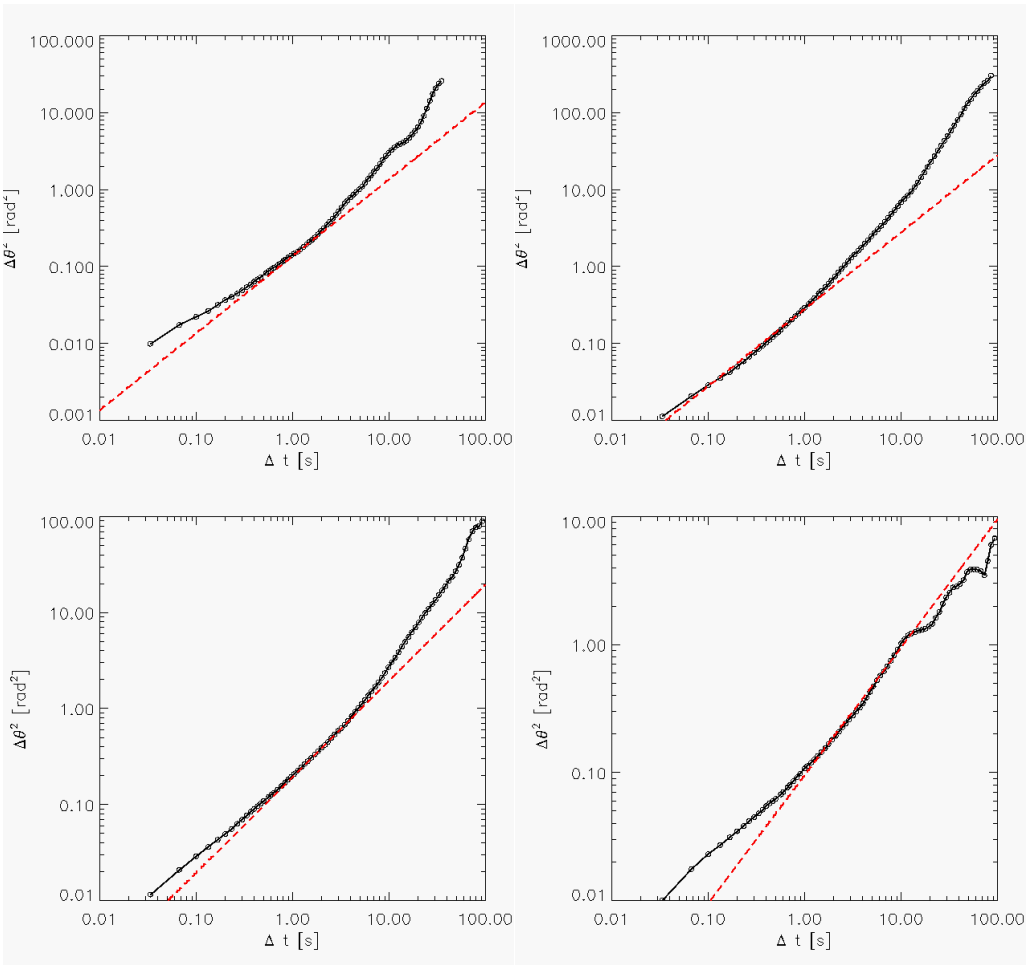

Figure 3.20: Fits made on the MSAD plots with φ= 0.60.

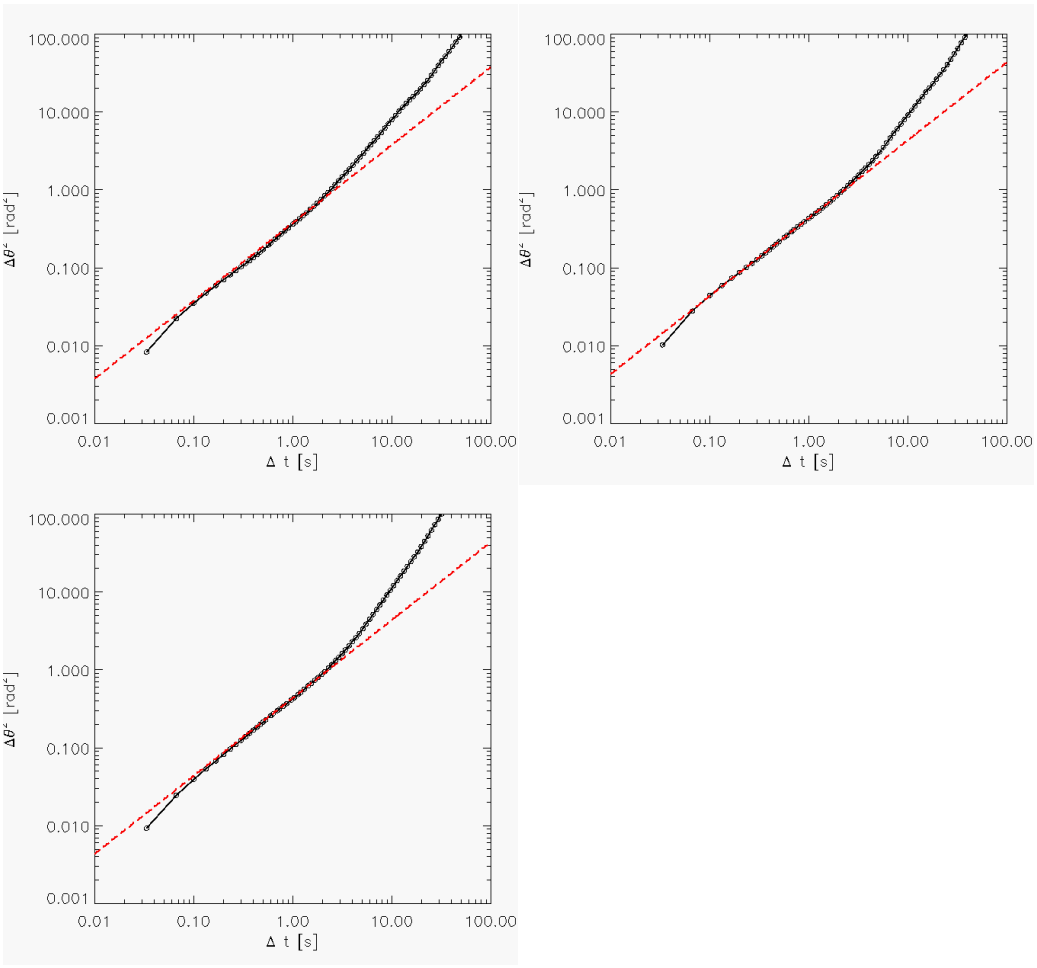

Figure 3.21: Fits made on the MSAD plots with φ= 0.57.

Once the fittings are complete and we obtain the desired D_T's and D_R's, we can then plot the ratio of these values to see whether or not the two motions decouple. Figure 3.22 plots the ratio of the diffusion coefficients as a function of volume fraction for 24 data sets. Overall, the points seem to show a slight upward trend as you move towards the right, which suggests that the clusters are exhibiting decoupled motion. If this system were coupled, all the points would fall along the red dashed line on Fig. 3.22.

To see what happens if I were to average the values, I calculated the average ratio for data points from the same calculated φ and plotted them in Fig. 3.23. Here, the upward trend seems

to be more convincing, but I think we need more data to confirm that the system is fully decoupled. The upward trend in these results is promising, because it goes to show that if we were able to physically increase the area fraction, which is difficult because more particles do not fit on the dish, we could see a more pronounced upward trend in the data.

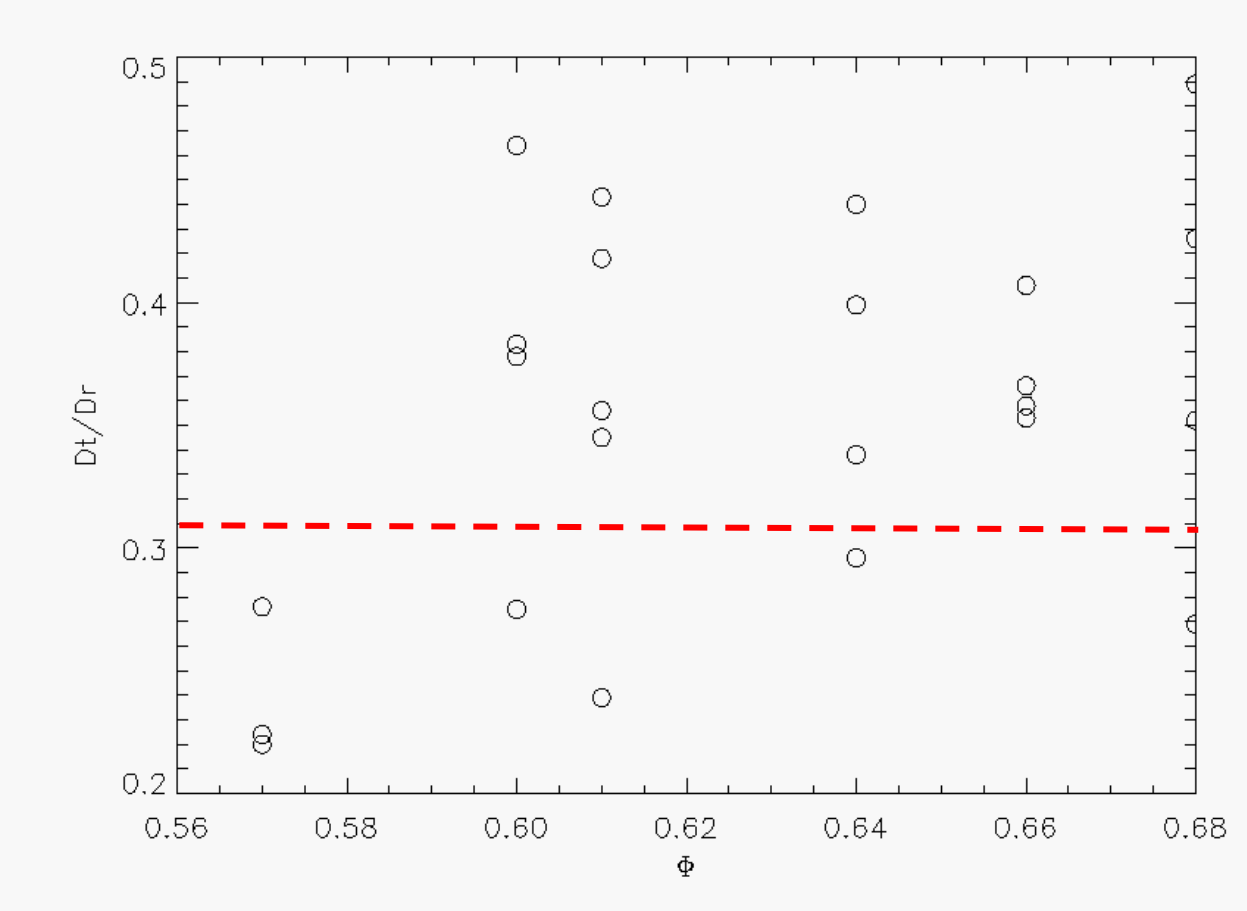

Figure 3.22: D_T/D_R for 24 datasets. The red dotted indicates what D_T/D_R would look like if the system were coupling.

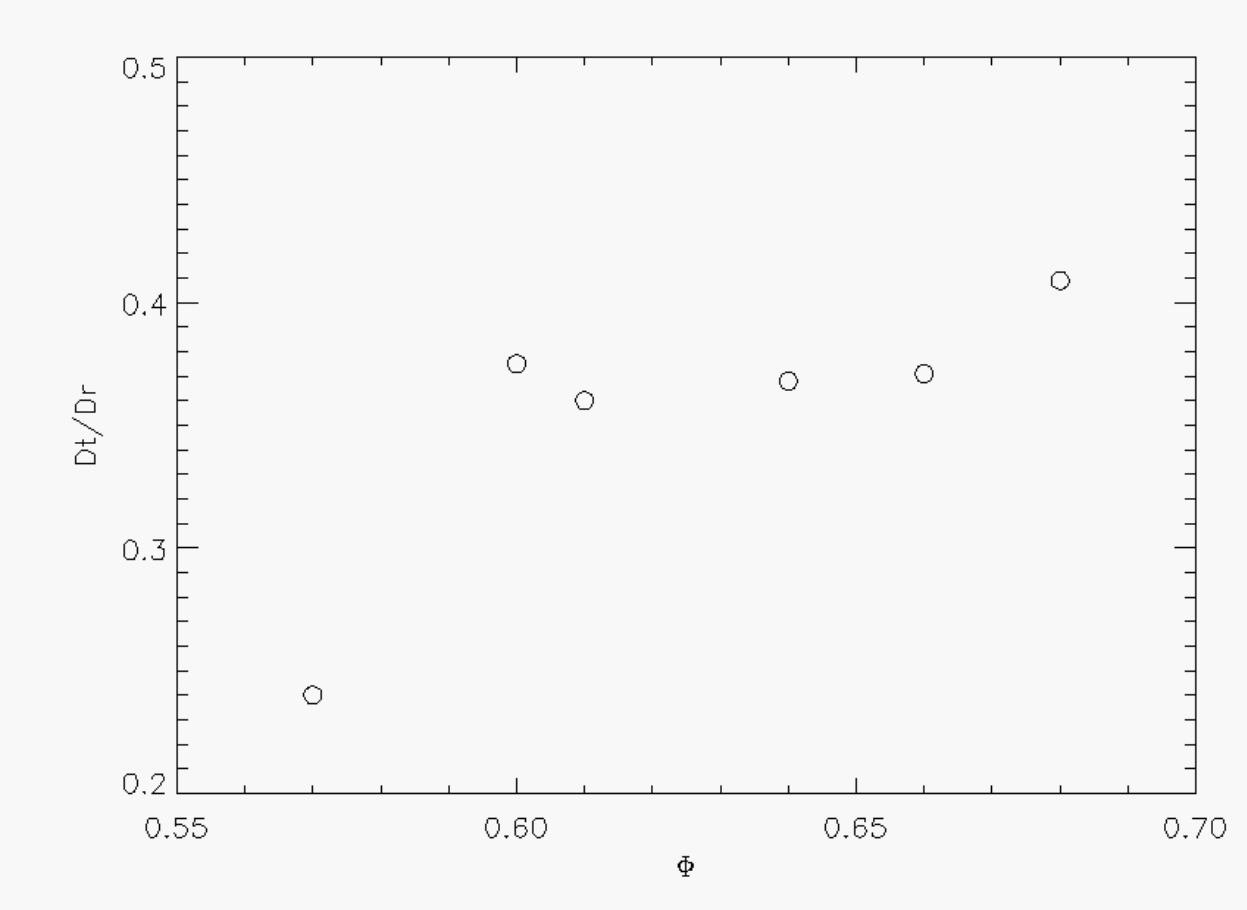

Figure 3.23: Averaged for each group of volume fraction.

3.3 Conclusion

In this experiment, I was successfully able to build a granular shaker system from scratch to study the two-dimensional rotational and translational diffusion of granular trimers in a sea of binary disks. The goal for this experiment was to see how different the translational and rotational components of diffusion changed with the area fraction of the system. I collected data in tiff format and used IDL to track and analyze the motions of the diffusing trimers in different area fractions. The trimers were undergoing translational cage breaking motion in the system and the cage breaks became more obvious as more particles were added to the system to increase the area fraction. The trimers were also found to go through cage breaks in their

angular motion. The mean square displacement (MSD) and mean square angular displacement (MSAD) of the trimers showed a dramatic fall as the area fraction was increased, similar to what can be seen in glassy systems approaching the glass transition. The ratio of D_T of D_R grew as area fraction of the system was increased, implying that the particles were translating faster than they were rotating, which is an interesting behavior known as decoupling. However, more data is needed to fully confirm this idea because noise could be influencing the behavior of the cluster.

Even though this experiment achieved the initial goal we had in mind, we did face some experimental difficulties that need to be improved upon. One of the biggest hurdles was obtaining a dish of uniformly diffusing particles on the loudspeaker. If you look back at Fig. 3.5, you will see a ring of stuck particles on around the edge of the dish with smallest area fraction. This was happening because the energy from the shaker was not transmitting uniformly to all the particles outside a central ring of particles, with about a 10 cm diameter from the center of the dish, which means that the trimer's diffusion was influenced by its location within the dish. This means that none of the area fractions I used above are fully accurate because we do not know the effective area fraction immediately surrounding a cluster. Another bigger question to consider is whether or not these kinds of experiments are worth doing at all, considering that it is nearly impossible to rule out all external sources of noise and error in the system, such as the stuck particles in my experiment and the non-uniform distribution of forces through the plate. Perhaps the best way to test these hypotheses is by using computer simulations because we can actually get our system to be as perfect as possible.

This experiment was designed to be a "proof of principle" experiment to test whether or not rotational and translational diffusions decouple in a very simple system. This experiment essentially used a loudspeaker to shake a dish of particles and see hints of the decoupling

effect, which was an exciting find for us because we were able to replicate the effect with a very basic model. This means that we can diversify this experiment to study other particle shapes diffusing while surrounded by a variety of different particle types in the future. This experiment taught me that interesting phenomena can be repeated in the simplest of experiments, and that it is important for us as scientists to take a step back and remove the extra fluff surrounding our experiments to prove very fundamental ideas.

Chapter 4

Conclusion

Even though we use "jammed" materials such as glass, plastic or Styrofoam on an everyday basis, it is fascinating to realize that we still do not really understand why these materials get jammed. Our goal is to understand the jamming transition better, and I did two experiments to stretch our understanding of different features of the jamming transition. For the first experiment I studied how tiny, micro-sized beads can feel the effects of being confined within a never-before-studied cylindrical geometry. Different features of the system such as the number density, distance from the boundary and size of the cylinder all intricately weave together to affect how the particles move around. For my second experiment, I used a system about 10,000 times larger than my colloids to study how clusters of particles translate faster than they rotate at higher volume fractions. The beauty of this experiment was that it was able to show this fascinating decoupling effect in as simple model system of disks being shaken by a speaker. Even though the jamming transition is rich in all of its complexity, we can still find new and exciting ways to push the envelope on what we know and what we do not know about jamming, and both of these experiments are examples of that.

The confinement experiment had interesting results that are new additions to the landscape of confinement studies done with colloids. I saw that confinement sllows down the mobility of

particles significantly in my mobility vs. radius plot, and the 2D geometry gives us new knowledge about the dynamics underlying confined samples. The layering of particles play an important role in controlling the dynamics of the sample, and the size of the tube plays a very important role in every experiment.The three different MSD three components slow down dramatically on getting closer to the boundary. The axial component is the slowest and peaks and dips the most in large tubes, and the fluctuations are closely related to the layers forming in the tube. In the smaller tube, the layers form from the center to the wall of the tube, which greatly affects all three components of the MSD, especially the radial, meaning that moving between layers is most difficult for the particles. All these results show that confinement truly does change how glassy materials behave in interesting ways.

In order to further analyze the data, we used an exponential fit and three new parameters to understand the mobility of the particles. These plots showed that ss the tube radius grows, the boundary becomes more important in affecting the overall mobility of particles and the particles must be closer to the boundary to feel its effects. Examining how these parameters change with volume fraction revealed interesting trends: when volume fraction is increased, the plateau value increases, the boundary had a more pronounced effect on the mobilty and the particles far away feel the effects of the boundary more. However, the bulk mobility increases with the tube radius, which was not expected, so this parameter is really a plateau instead of a bulk value.

In the second experiment, I built a granular shaker system from scratch to study the two-dimensional rotational and translational diffusion of granular trimers in a sea of binary disks. This experiment was a "proof of principle" experiment to see whether or not rotational and translational diffusions decouple in the most simple system we could think of. The trimers were undergoing translational and angular cage breaking motion and the translational cage breaks

became more visible as the volume fraction was increased. The mean square displacement (MSD) and mean square angular displacement (MSAD) of the trimers slowed down greatly with a growing area fraction, just like it does in glassy systems. The ratio of D_T of D_R appeared to increase at higher area fractions, implying slower rotation than translation, which is the decoupling effect we were looking for. However, more data is needed to fully confirm this idea because noise could be influencing the behavior of the cluster.

References

M. Alcoutlabi and G. B. McKenna, "Effects of confinement on material be- haviour at the nanometre size scale," J. Phys.: Cond. Matt., vol. 17, pp. R461– R524, Apr. 2005.

B. J. Alder, D. M. Gass, and T. E. Wainwright,"Studies in Molecular Dynamics. VIII. The Transport Coefficients for a Hard-Sphere Fluid," J. Chem. Phys. 53, 3813 (1970).

L. Antl, J. W. Goodwin, R. D. Hill, R. H. Ottewill, S. M. Owens, S. Papworth, and J. A. Waters, "The preparation of poly(methyl methacrylate) latices in non-aqueous media," Colloids and Surfaces, vol. 17, pp. 67–78, Jan. 1986.

I. Chang, F. Fujara, B. Geil, G. Heuberger, T. Mangel, and H. Sillescu, "Trans- lational and rotational molecular motion in supercooled liquids studied by NMR and forced rayleigh scattering," J. Non-Cryst. Solids, vol. 172-174, pp. 248–255, 1994.

J. Crocker, "Methods of digital video microscopy for colloidal studies," J. Colloid Interf. Sci., vol. 179, pp. 298–310, Apr. 1996.

K. W. Desmond and E.R. Weeks, "Random close packing of disks and spheres in confined geometries," Phys. Rev. E 80, 051305 (2009).

P. G. Debenedetti and F. H. Stillinger, "Supercooled liquids and the glass transition," Nature, vol. 410, pp. 259–267, Mar. 2001.

M. D. Ediger, "Spatially heterogeneous dynamics in supercooled liquids," Annual Review of Physical Chemistry, vol. 51, pp. 99–128, Oct. 2000.

A. Einstein, "On the movement of small particles suspended in a stationary liquid demanded by the molecular-kinetic theory of heat," Annalen der Physik (Leipzig), vol. 17, pp. 549–560, 1905.

K. V. Edmond, C. R. Nugent, and E. R. Weeks, "Local influence of boundary conditions on a confined supercooled colloidal liquid", The European Physical Journal - Special Topics 189(1):83-93, March 2010.

P. Habdas and E. R. Weeks, " Video Microscopy of Colloidal Suspensions and Colloidal Crystals", Current Opinion in Colloid and Interface Sci. 7, 196-203 (2002).

M. Holz, X. Mao, D. Seiferling, and A. Sacco, "Experimental study of dynamic isotope effects in molecular liquids: Detection of translation-rotation coupling", J. Chem. Phys. 104 669, 1996.

G. L. Hunter & E. R. Weeks, "Free energy landscape for cage breaking of three hard disks," Phys. Rev. E 85, 031504 (2012).

S. Kim, C.B. Roth, and J.M. Torkelson, "Effect of Nanoscale Confinement on the Glass Transition Temperature of Free-Standing Polymer Films: Novel, Self-Referencing Fluorescence Method," J. Polym. Sci., Part B: Polym. Phys. 2008, 46, 2754-2764.

C. R. Nugent, K. V. Edmond, H. N. Patel, and E. R. Weeks, "Colloidal glass transition observed in confinement", Physical Review Letters, 99(2):025702, 2007.

V. Prasad, D. Semwogerere, and E. R. Weeks, "Confocal microscopy of colloids," J. Phys.: Cond. Matt., vol. 19, p. 113102, Mar. 2007.

P. Scheidler, W. Kob, and K. Binder, "Cooperative motion and growing length scales in supercooled confined liquids," EPL (Europhysics Letters), vol. 59, pp. 701–707, Sept. 2002.

K. S. Schweizer and E. J. Saltzman, "Entropic barriers, activated hopping, and the glass transition in colloidal suspensions", J. Chem. Phys. 119, 1181 (2003).

R. J. Speedy, "The hard sphere glass transition", Molecular Physics, Vol. 95, Iss. 2, 2009.

W. Sutherland, "A dynamical theory of diffusion for non-electrolytes and the molecular mass of albumin," Phil. Mag., vol. 9, pp. 781–785, 1905.

E. R. Weeks and D. A. Weitz, "Properties of cage rearrangements observed near the colloidal glass transition," Phys. Rev. Lett., vol. 89, p. 095704, Aug. 2002.

E. R. Weeks and D. A. Weitz, "Subdiffusion and the cage effect studied near the colloidal glass transition," Chem. Phys., vol. 284, pp. 361–367, Nov. 2002.

Marcus T. Cicerone and M. D. Ediger, "Enhanced translation of probe molecules in supercooled o-terphenyl: Signature of spatially heterogeneous dynamics?", J. Chem. Phys. 104, 7210, 1996.

E. R. Weeks, **"**Microscopy of soft materials**",** book chapter in Experimental and Computational Methods in Soft Condensed Matter, ed. JS Olafsen, Cambridge University Press, 2010).

E. R. Weeks and D. A. Weitz, "Properties of cage rearrangements observed near the colloidal glass transition," Phys. Rev. Lett., vol. 89, p. 095704, Aug. 2002.

E. R. Weeks, "Soft jammed materials", book chapter in Statistical Physics of Complex Fluids, pp. 2-1 -- 2-87, eds. S Maruyama & M Tokuyama (Tohoku University Press, Sendai, Japan, 2007.

L. V. Woodcock, "Glass transition in the hard-sphere model and Kauzmann's Paradox. "Annals of the New York Academy of Sciences, 371: 274–298 (1981).